

1 **Serum proteomic profiling of physical activity reveals CD300LG as a novel exerkin with a**
2 **potential causal link to glucose homeostasis**

3 Sindre Lee-Ødegård^{1,2}, Marit Hjorth^{3*}, Thomas Olsen^{3*}, Gunn-Helen Moen^{2,4,5,7}, Emily
4 Daubney⁴, David M Evans⁴⁻⁶, Andrea Hevener⁸, Aldons Jake Lusi^{9,10}, Mingqi Zhou¹¹, Marcus
5 Michael Seldin¹¹, Hooman Allayee^{12,13}, Jonas Krag Viken², Hanne L. Gulseth¹⁴, Frode
6 Norheim³, Christian A. Drevon¹⁵, Kåre I. Birkeland^{1,2}

7 ¹Department of Endocrinology, Morbid obesity and Preventive Medicine, Oslo University Hospital, Norway.

8 ²Institute of Clinical Medicine, Faculty of Medicine, University of Oslo, Norway.

9 ³Department of Nutrition, Institute of Basic Medical Sciences, Faculty of Medicine, University of Oslo, Norway.

10 ⁴Institute for Molecular Bioscience, The University of Queensland, Brisbane, Australia

11 ⁵The Frazer Institute, The University of Queensland, 4102, Woolloongabba, QLD, Australia.

12 ⁶MRC Integrative Epidemiology Unit, University of Bristol, Bristol, UK.

13 ⁷Department of Public Health and Nursing, K.G. Jebsen Center for Genetic Epidemiology, NTNU, Norwegian
14 University of Science and Technology, Trondheim, Norway.

15 ⁸Division of Endocrinology, Department of Medicine, David Geffen School of Medicine, University of California
16 at Los Angeles, Los Angeles, California.

17 ⁹Department of Human Genetics, UCLA, Los Angeles, CA, USA.

18 ¹⁰Division of Cardiology, Department of Medicine, David Geffen School of Medicine at UCLA, Los Angeles, CA,
19 USA.

20 ¹¹Department of Biological Chemistry, University of California, Irvine, Irvine, USA.

21 ¹²Departments of Population & Public Health Sciences, Keck School of Medicine, University of Southern
22 California, Los Angeles, USA.

23 ¹³Department of Biochemistry & Molecular Medicine, Keck School of Medicine, University of Southern
24 California, Los Angeles, USA.

25 ¹⁴Department of Chronic Diseases and Ageing, Norwegian Institute of Public Health, Norway.

26 ¹⁵Vitas Ltd, Oslo Science Park, Oslo, Norway.

27 *Shared second authorship

28

29 Correspondence: Sognsvannsveien 9, Domus Medica, 0372 Oslo, Norway. Email:
30 sindre.lee@medisin.uio.no. Phone: +47 22 85 13 92. Fax: + 47 22 85 03 01.

31

32

33

34

35 **Abstract**

36 **Background:** Physical activity has been associated with preventing the development of type
37 2 diabetes and atherosclerotic cardiovascular disease. However, our understanding of the
38 precise molecular mechanisms underlying these effects remains incomplete and good
39 biomarkers to objectively assess physical activity are lacking.

40 **Methods:** We analyzed 3072 serum proteins in 26 men, normal weight or overweight,
41 undergoing 12 weeks of a combined strength and endurance exercise intervention. We
42 estimated insulin sensitivity with hyperinsulinemic euglycemic clamp, maximum oxygen
43 uptake, muscle strength, and used MRI/MRS to evaluate body composition and organ fat
44 depots. Muscle and subcutaneous adipose tissue biopsies were used for mRNA sequencing.
45 Additional association analyses were performed in samples from up to 47,747 individuals in
46 the UK Biobank, as well as using 2-sample Mendelian randomization and mice models.

47 **Results:** Following 12 weeks of exercise intervention, we observed significant changes in 283
48 serum proteins. Notably, 66 of these proteins were elevated in overweight men and
49 positively associated with liver fat before the exercise regimen, but were normalized after
50 exercise. Furthermore, for 19.7% and 12.1% of the exercise-responsive proteins,
51 corresponding changes in mRNA expression levels in muscle and fat, respectively, were
52 shown. The protein CD300LG displayed consistent alterations in blood, muscle, and fat.
53 Serum CD300LG exhibited positive associations with insulin sensitivity, and to angiogenesis-
54 related gene expression in both muscle and fat. Furthermore, serum CD300LG was positively
55 associated with physical activity and negatively associated with glucose levels in the UK
56 Biobank. In this sample, the association between serum CD300LG and physical activity was
57 significantly stronger in men than in women. Mendelian randomization analysis suggested
58 potential causal relationships between levels of serum CD300LG and fasting glucose, 2-hour
59 glucose after an oral glucose tolerance test, and HbA1c. Additionally, Cd300lg responded to
60 exercise in a mouse model, and we observed signs of impaired glucose tolerance in male,
61 but not female, *Cd300lg* knockout mice.

62 **Conclusion:** Our study identified several novel proteins in serum whose levels change in
63 response to prolonged exercise and were significantly associated with body composition,
64 liver fat, and glucose homeostasis. Serum CD300LG increased with physical activity and is a

65 potential causal link to improved glucose levels. CD300LG may be a promising exercise
66 biomarker and a therapeutic target in type 2 diabetes.

67

68 **Introduction**

69 Physical activity is a cornerstone in the prevention and treatment of several chronic diseases
70 like obesity, non-alcoholic fatty liver disease (NAFLD), atherosclerotic vascular disease, and
71 type 2 diabetes mellitus ¹. Both acute and long-term exercise may enhance insulin sensitivity
72 and thereby improve glucose tolerance ². Both resistance and endurance exercises enhance
73 insulin sensitivity, although the most pronounced effect is observed when combining these
74 training modalities ³.

75

76 Metabolic adaptations to exercise encompass intricate inter-organ communication
77 facilitated by molecules referred to as exer kines ⁴⁻⁷. These exer kines are secreted from
78 various tissues and include a variety of signal molecules released in response to acute
79 and/or long-term exercise with endocrine, paracrine and/or autocrine functions ^{4,5}. Although
80 there has been considerable emphasis on exer kines originating from skeletal muscle (SkM)
81 ^{8,9}, it is also known that exer kines can originate from organs such as white ^{6,10,11} and brown
82 adipose tissue ¹² or the liver ¹³. The established *bona fide* exer kine, interleukin-6 (IL6), is
83 released during muscle contractions, contributing to improved overall glucose homeostasis
84 ^{4,14}. In addition, a range of other exer kines are recognized, including IL7 ¹⁵, 12,13-diHOME ¹²,
85 myonectin ¹⁶, myostatin ^{17,18}, METRNL ¹⁹, CSF1 ⁸, decorin ²⁰, SFRP4 ¹⁰, fetuin-A ^{13,21}, and
86 ANGPTL4 ^{22,23}, among many others ⁵.

87

88 Extensive screening aimed at discovering novel exercise responsive blood proteins have
89 faced considerable challenges, primarily due to the technical challenges in quantifying the
90 blood proteome on a large scale. However, recent advances in multi-plex technology, such as
91 the proximity extension assay (PEA), have made it possible to quantify more than 3000
92 proteins in blood samples more reliably than traditional untargeted mass spectrometry
93 (<https://olink.com/application/pea>). Some recent studies have used other proteomic
94 platforms, such as aptamer-based techniques (<https://somalogic.com/somascan-platform/>),
95 to show that acute and long-term aerobic exercise affected several hundred serum proteins

96 ²⁴⁻²⁸, but the downstream causal effects of such changes on clinical phenotypes are not
97 known. Furthermore, no studies have used the PEA technology to identify exerkinases
98 potentially underlying the mechanisms through which long-term physical activity, including
99 strength exercise, enhances glucose homeostasis.

100

101 We performed the ‘physical activity, myokines and glucose metabolism’ (MyoGlu) study ²⁹,
102 which was a controlled clinical trial aiming to identify novel secreted factors (‘exerkinases’)
103 that may serve as links between physical activity and glucose metabolism. We conducted a
104 comprehensive serum screening of 3072 proteins in normal weight and overweight men
105 both before and after combined endurance and strength exercise. Rigorous phenotyping was
106 carried out, including hyperinsulinemic euglycemic clamping, assessments of maximum
107 oxygen uptake, maximum muscle strength, and ankle-to-neck MRI/MRS scans.

108

109 Exerkinases identified with potential effects on glucose homeostasis in the MyoGlu study were
110 subsequently subject to analysis across several external data sets. Using data from 47,747
111 participants in the UK Biobank ³⁰, we assessed correlations between candidate proteins and
112 estimates of physical activity and glucometabolic outcomes. These associations were then
113 tested for causality using Mendelian randomization (MR). Exerkinases of interest were also
114 assessed in a knockout mouse model and in an exercise mouse model to further assess
115 potential links with glucose homeostasis.

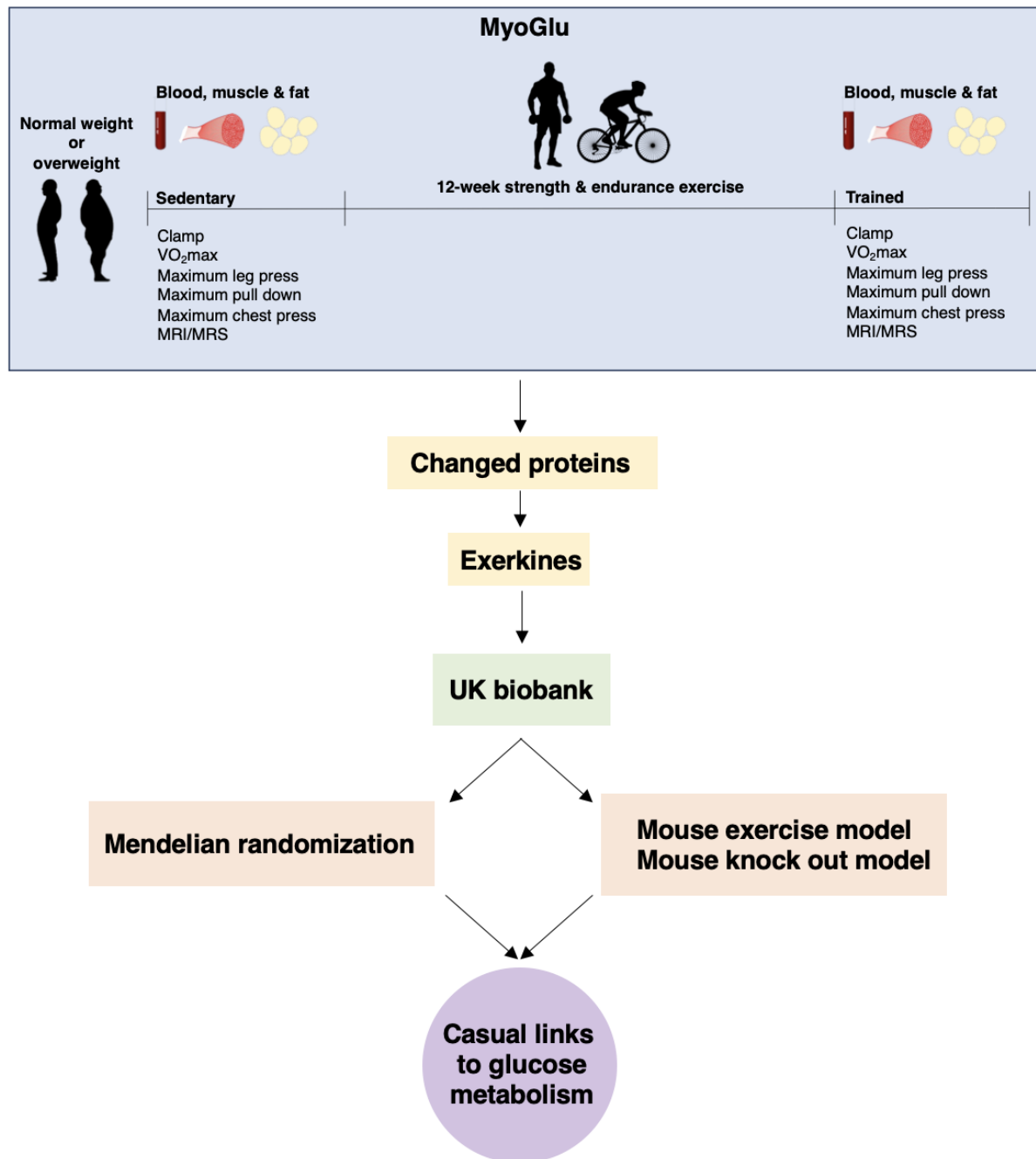
116

117 **Results**

118 **Cohort characteristics**

119 We studied 26 male participants, including 13 with normal weight, and another 13 with
120 overweight, as described previously ²⁹. They were subjected to 12-weeks of high-intensity
121 resistance and endurance exercise (Figure 1). The overweight participants had lower glucose
122 tolerance and insulin sensitivity compared to the normal weight participants
123 (Supplementary Table 1). After the 12-week intervention, body fat mass decreased and lean
124 body mass increased, together with significant improvements in insulin sensitivity (~40%),
125 maximum oxygen uptake and muscle strength in both groups (Supplementary Table 1).

126



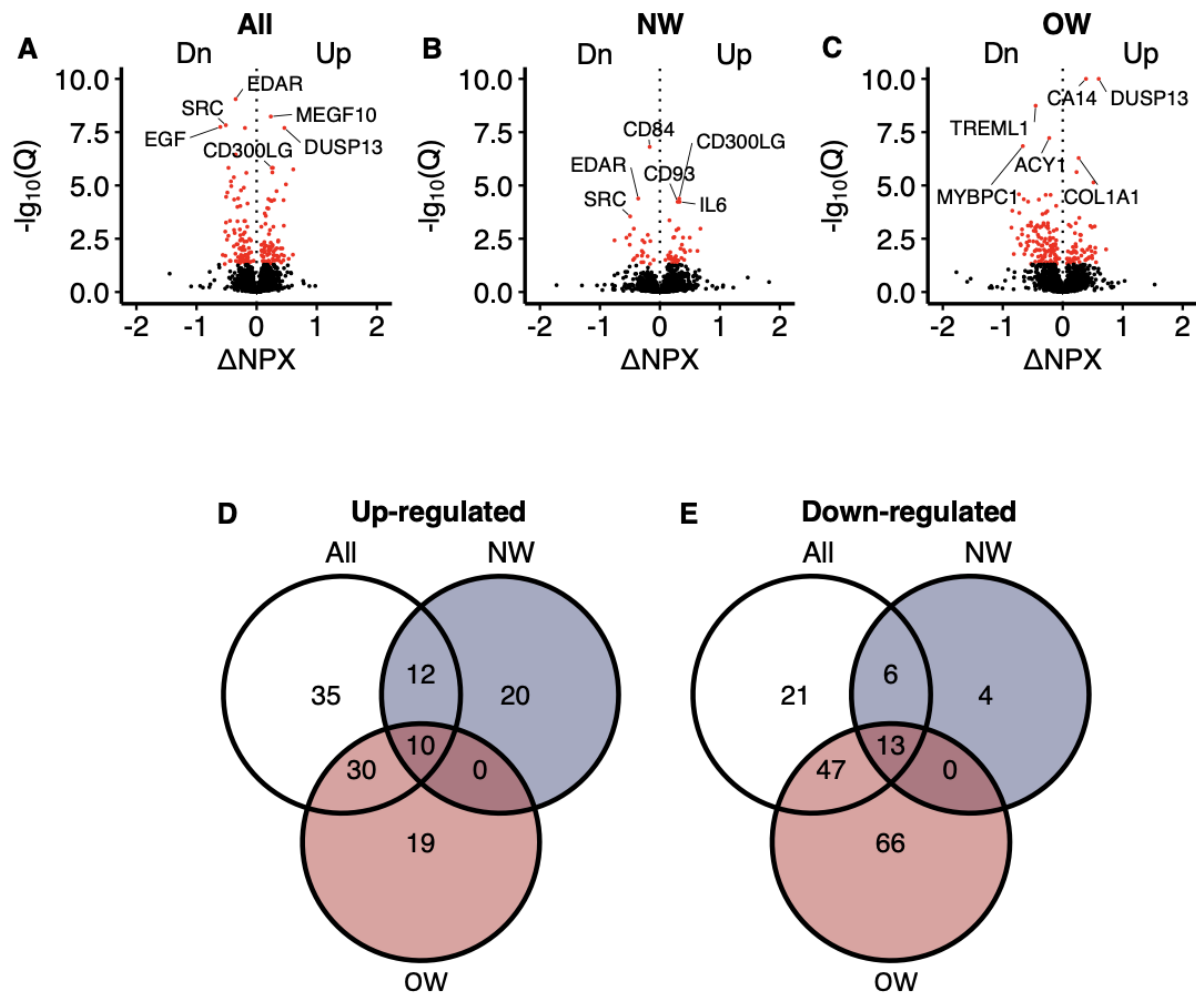
127

128 **Figure 1. Study overview.** We recruited sedentary men with either normal weight or
129 overweight for deep phenotyping before and after a prolonged exercise intervention. Multi-
130 omic analyses, including serum proteomics, clinical traits and muscle and fat transcriptomics
131 identified changed proteins and potential exerkines. Candidate exerkines were subsequently
132 analyzed in serum samples from the UK biobank and tested for associations with physical
133 activity and glucometabolic traits. Top candidates were then subjected to Mendelian
134 randomization and investigated in a mouse exercise model and in a mouse knock-out model
135 to assess casual links between exerkines and glucometabolic traits.

136 **Serum proteome responses to prolonged exercise**

137 Recognizing that circulating proteins could mediate exercise-induced metabolic
138 improvements, we next investigated alterations in the serum proteome in response to the
139 12-week intervention using PEA technology. Of the 3072 proteins quantified, we detected
140 increased serum concentrations of 126 proteins, and decreased serum concentrations of
141 157 proteins following the 12-week intervention, at a false discovery rate (FDR) below 5%
142 (Figure 2 A-C; Supplementary Table 2-4). Among these, 20 proteins increased exclusively in
143 normal weight men, whereas 19 proteins increased exclusively in overweight men (Figure 2
144 D). Four proteins were uniquely reduced in normal weight men, and 66 proteins were
145 uniquely reduced in overweight men (Figure 2 E).

146



147

148 **Figure 2. Serum proteomic responses to prolonged exercise.** (A) A volcano plot showing
 149 responses in all participants. The X-axis shows $\log_2(\text{fold-changes})$ and the Y-axis shows
 150 negative $\log_{10}(Q\text{-values})$. The red dots indicate statistical significance ($Q < 0.05$). Only the top
 151 3 up/down-regulated proteins are annotated. (B-C) Similar to A, but in normal weight and
 152 overweight men only. (D-E) Venn diagrams of the significant change in proteins shown in A-
 153 C. NPX = normalized protein expression. Q = P-values corrected using Benjamini-Hochberg's
 154 method. NW = normal weight. OW = overweight.

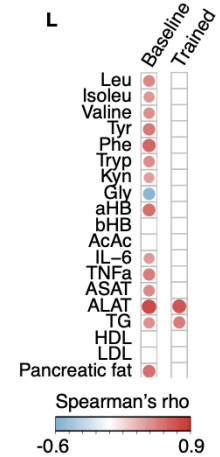
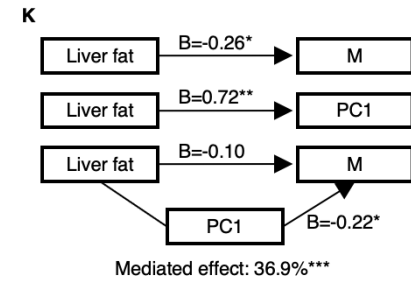
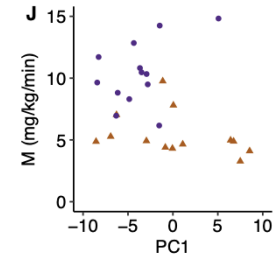
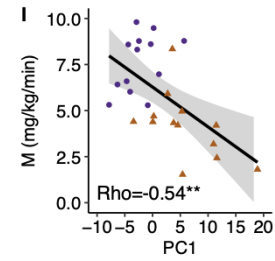
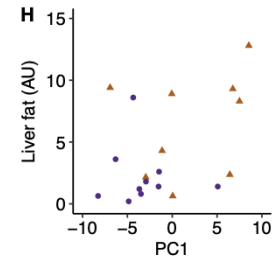
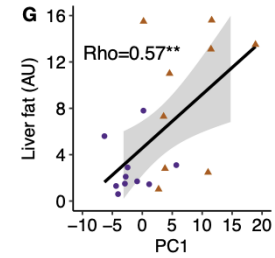
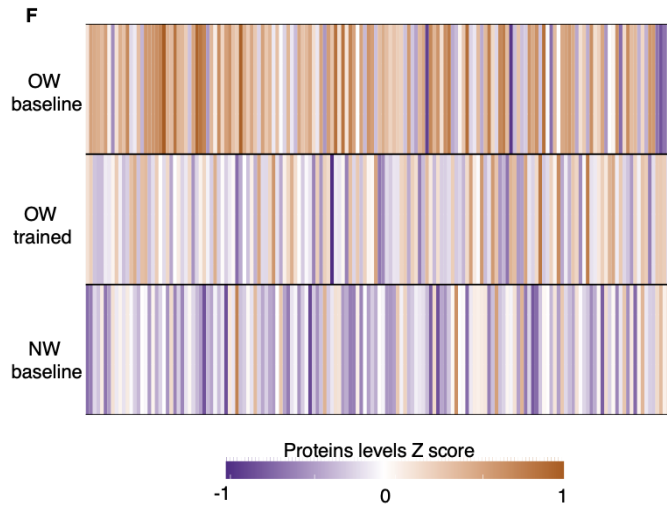
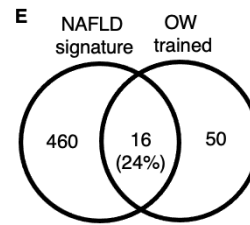
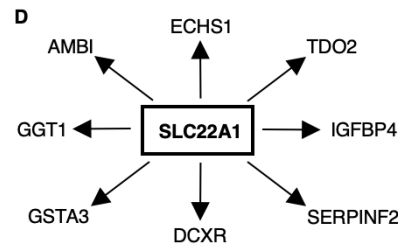
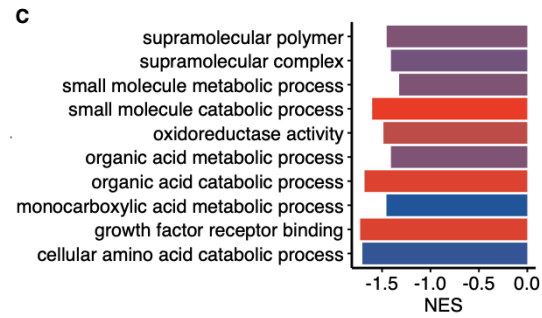
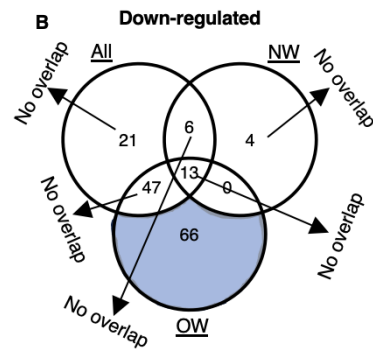
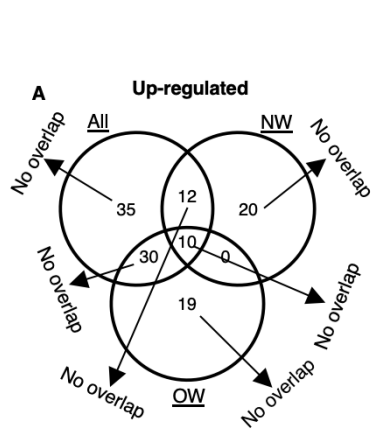
155 Several of the exercise-responsive proteins had potential roles in muscle adaptation and
156 metabolism. For example, platelet-derived growth factor subunit B (PDGFB) and IL7, are
157 both myokines with potential effects on muscle differentiation ^{15,31}. Further, fibroblast
158 growth factor-binding protein 3 (FGFBP3) may influence running capacity ³² and muscle
159 strength ³³. NADH-cytochrome b5 reductase 2 (CYB5R2) can preserve SkM mitochondria
160 function in aging mice ³⁴. FGFBP3 and switch-associated protein 70 (SWAP70) may protect
161 against weight gain ³⁵ and cardiac hypertrophy ³⁶, respectively. Finally, dual specificity
162 protein phosphatase 13 isoform A (DUSP13A) is highly specific to SkM ³⁷, making it a
163 potential novel muscle-specific marker for long-term exercise. Detailed results for 2885
164 proteins in response to prolonged exercise are shown in Supplementary Table 2.

165

166 **A proteomic liver fat signature in overweight men**

167 In response to the 12-week exercise intervention, a larger number of serum proteins
168 responded in overweight men than in normal weight men (Figure 2 B-C). In particular, 66
169 proteins decreased in serum after 12 weeks in overweight men (Figure 2 E). Gene ontology
170 analyses revealed known pathways only for the proteins that decreased in overweight men
171 (Figure 3 A-B), and one of the most enriched pathways is related to metabolism of organic
172 acids (Figure 3 C). A key driver analysis of the 66 proteins identified SLC22A1, a hepatocyte
173 transporter related to liver fat content (Figure 3 D). Furthermore, the 66 proteins also
174 displayed a 24% overlap with a known human serum proteomic signature of non-alcoholic
175 fatty liver disease (NAFLD; Figure 3 E) ³⁸, but no common proteins with signatures of specific
176 liver cells (The Human Liver Cell Atlas: ³⁹). Baseline serum protein concentrations in the
177 identified signature of 66 proteins were higher among men with overweight compared to
178 those with normal weight, but were reduced or normalized in overweight men following
179 prolonged exercise (Figure 3 F). Using principal component analysis of the 66 proteins, the
180 first component correlated positively to liver fat content at baseline (Figure 3 G), but not
181 after prolonged exercise (Figure 3 H). Similarly, the first component also correlated positively
182 with several liver-related markers at baseline (Figure 3 L) and negatively to insulin sensitivity
183 at baseline (Figure 3 I), but not after prolonged exercise (Figure 3 J). The first component
184 mediated 37% of the association between baseline insulin sensitivity and liver fat content
185 (Figure 3 K).

186

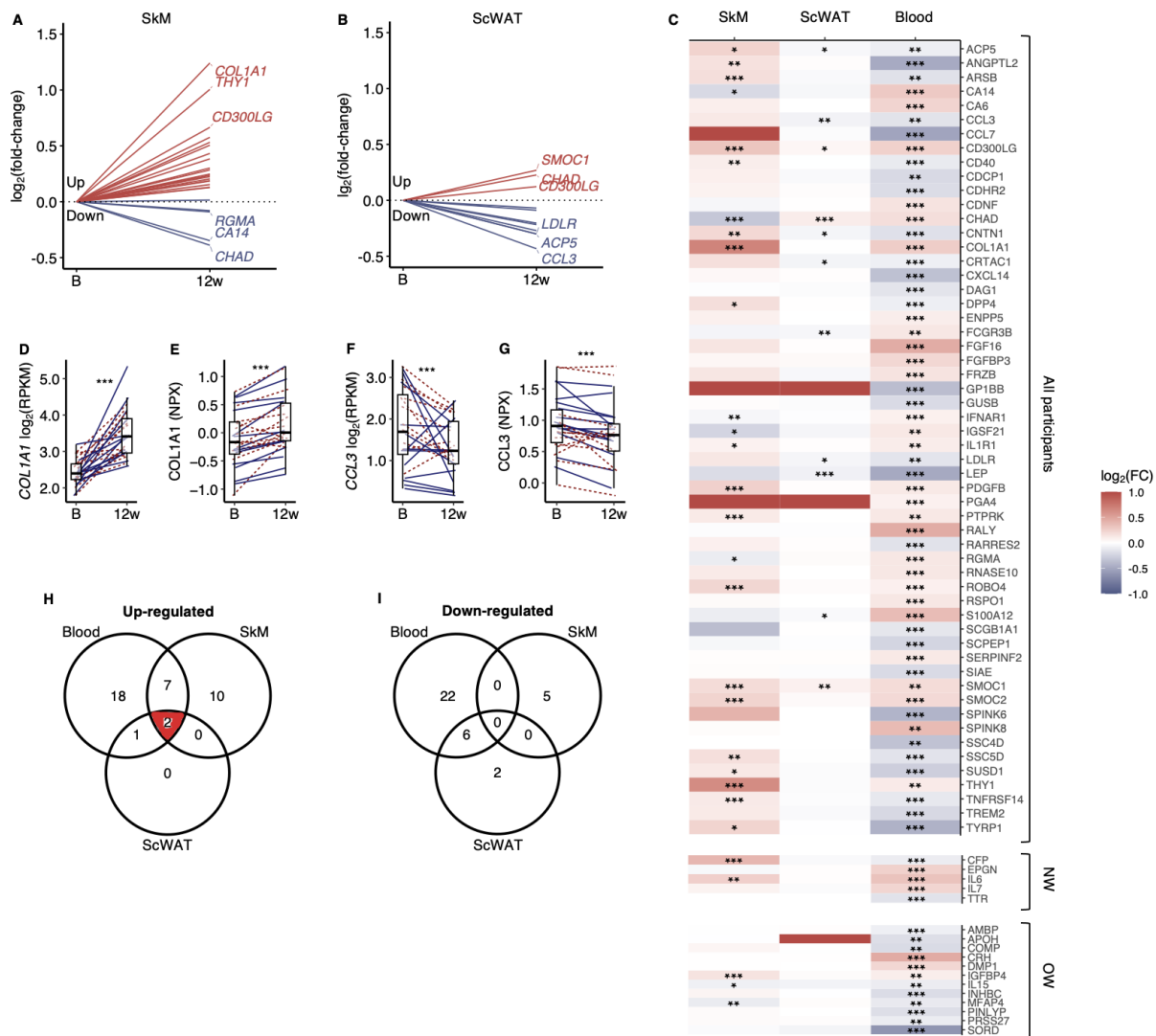


188 **Figure 3. A serum proteomic liver fat signature.** (A) No up-regulated proteins after prolonged exercise overlapped with known pathways. (B)
189 Only the 66 down-regulated proteins in the OW group overlapped with known pathways. (C) Top 10 gene sets overlapping with these 66
190 proteins. (D) SLC22A1 is a key driver among these 66 proteins. (E) These 66 proteins overlapped with a known human serum proteomic non-
191 alcoholic fatty liver disease signature from Govaere et al³⁸. (F) The down-regulated proteins in the OW group were elevated in OW vs. NW at
192 baseline but normalized in the OW group after prolonged exercise. The principal component of these 66 proteins correlated with (G) liver fat
193 content at baseline, but (H) not after prolonged exercise, with (I) the clamp M value at baseline, but (J) not after prolonged exercise. (K) The
194 principal component (PC) of these 66 proteins mediated 36.9% of the association between liver fat and M. (L) The principal component of these
195 66 proteins correlated with several liver-related markers at baseline, but not after prolonged exercise except for ASAT and ALAT (white = non-
196 significant, red/blue = significant). * $p < 0.05$ and ** $p < 0.01$.

197 **Secretory proteins**

198 Among the 96 up-regulated and 110 down-regulated serum proteins responding to the 12-
199 week exercise intervention (Figure 2 D-E), 37 are curated secretory proteins, and another 46
200 proteins are predicted as highly likely secretory proteins (Figure 4 A-C). We assessed the
201 corresponding mRNA responses in SkM and subcutaneous white adipose tissue (ScWAT)
202 following the 12-week intervention (Figure 4 A-C). In total, 19.7 % of the serum secretory
203 proteins displayed a directionally consistent significant change mRNA levels in SkM, whereas
204 12.1 % of the serum secretory proteins exhibited a corresponding mRNA response in ScWAT
205 (Figure 4 C). *COL1A1* was the most responsive SkM mRNA that also had a corresponding
206 increase in serum *COL1A1* after prolonged exercise (Figure 4 D-E). *CCL3* was the most
207 responsive ScWAT mRNA that also had a corresponding decrease in serum after prolonged
208 exercise (Figure 4 F-G). To prioritize proteins for follow-up analyses, we focused on *SMOC1*
209 and *CD300LG*, which had similar exercise responses in blood, SkM and ScWAT (Figure 4 H).
210 *SMOC1* is a known hepatokine with effects on insulin sensitivity in mice⁴⁰, but probably with
211 no causal link to insulin sensitivity in humans^{40,41}. Thus, we focused on *CD300LG* in
212 subsequent analyses.

213

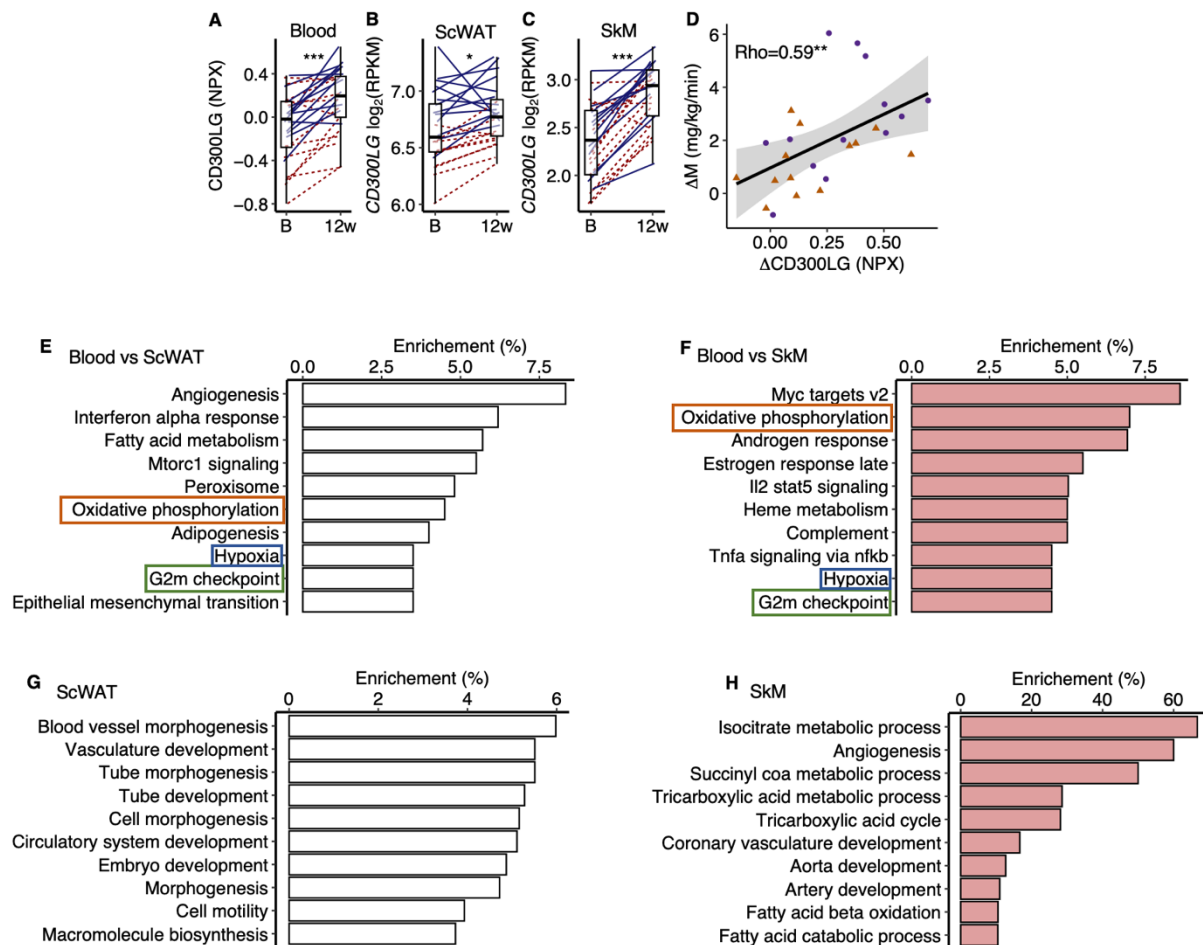


214
215 **Figure 4. Comparison of secretory protein responses to prolonged exercise in blood with**
216 **corresponding mRNA levels in skeletal muscle and adipose tissue. (A) mRNA levels in**
217 **skeletal muscle and (B) adipose tissue for proteins that responded significantly to prolonged**
218 **exercise. (C) A heatmap of $\log_2(\text{fold-changes})$ in blood, skeletal muscle and adipose tissue.**
219 **(D) The most responding mRNA in skeletal muscle, and (E) the response in the blood protein.**
220 **(F) The most responding mRNA in adipose tissue, and (G) the response in the blood. (H-I)**
221 **Venn diagrams of significant changes in blood, skeletal muscle and adipose tissue. FC = fold-**
222 **change. SkM = skeletal muscle. ScWAT = subcutaneous adipose tissue. NPX = normalized**
223 **protein expression. RPKM = reads per kilobase per million mapped read. * $p < 0.05$, ** $p < 0.01$**
224 **and *** $p < 0.001$.**
225

226 **CD300LG**

227 CD300LG displayed increased concentration in serum (+20%, $p < 0.001$) together with
228 increased levels in both SkM (+60%, $p < 0.001$) and scWAT (+13%, $p = 0.01$) mRNA following
229 the 12-week exercise intervention (Figure 5 A-C). Changes in serum CD300LG correlated
230 positively with changes in insulin sensitivity after the intervention ($\rho = 0.59$, $p = 0.002$; Figure
231 5 D). In addition, serum CD300LG concentration was lower in overweight than normal
232 weight men (-51%, $p = 0.014$) and positively correlated with insulin sensitivity before as well
233 as after the 12-week intervention (pre-trained: $r = 0.50$, $p = 0.001$, and post-trained: $r = 0.43$,
234 $p = 0.028$).

235



236

237

238 **Figure 5. CD300LG.** (A) The response from baseline to week 12 in serum CD300LG and

239 CD300LG mRNA in (B) subcutaneous adipose tissue (ScWAT) and (C) skeletal muscle (SkM).

240 (D) Correlation between the change from before to after prolonged exercise in serum

241 CD300LG and insulin sensitivity. Pathway enrichment analyses were performed on the top

242 500 most correlated (and $p < 0.05$) genes to the change in serum CD300LG, and only the top

10 pathways with $Q < 0.05$ are presented. * $p < 0.05$, ** $p < 0.01$ and *** $p < 0.001$.

243

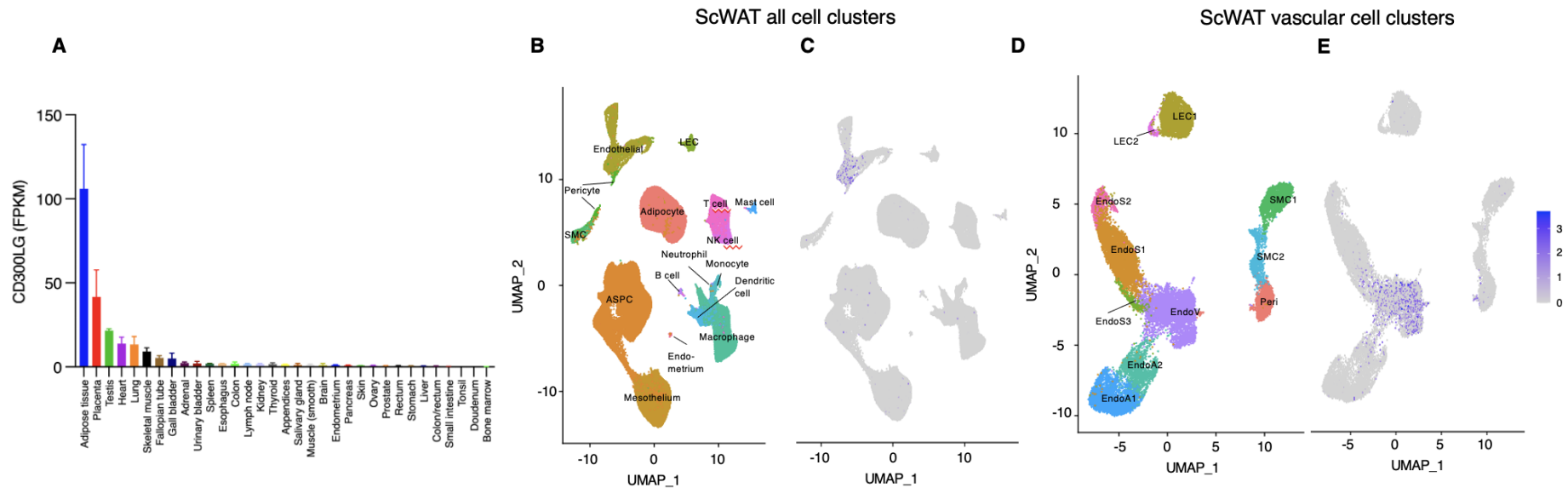
244

245 To investigate the potential effect of serum CD300LG on SkM and ScWAT, we performed an
246 overrepresentation analysis on the top 500 mRNAs that were positively correlated ($p < 0.05$)
247 with serum CD300LG levels in each tissue (Figure 5 E-H). Pathway analyses revealed that the
248 change in serum CD300LG concentrations correlated with changes in expression of genes
249 involved in oxidative phosphorylation, G2M check point and hypoxia both in ScWAT and SkM
250 (Figure 5 E-F). In ScWAT, serum CD300LG levels also showed the strongest enrichment with
251 angiogenesis pathways (Figure 5 E). In ScWAT, the change in ScWAT *CD300LG* mRNA levels
252 correlated positively with the change in ScWAT mRNA of genes related to
253 angiogenesis/vasculature development (Figure 5 G). Similar correlations between *CD300LG*
254 mRNA and angiogenesis genes were observed in SkM as well (Figure 5 H). For example, 60%
255 of the mRNAs in the angiogenesis pathway correlated with *CD300LG* (Figure 5 H). However,
256 serum CD300LG levels were also correlated positively with pathways related to fatty acid
257 metabolism in both ScWAT (Figure 5 E) and SkM (Figure 5 H).

258

259 To explore tissue specific expression of CD300LG, we utilized data from a publicly available
260 human tissue panel ⁴². CD300LG is highly expressed in adipose tissue compared to other
261 tissues (Figure 6 A) supporting our observation that ScWAT expression was substantially
262 higher than in SkM (Figure 5 B-C). To further investigate which cells in ScWAT that express
263 CD300LG, we utilized data from a single cell mRNA sequencing atlas of human ScWAT
264 (https://singlecell.broadinstitute.org/single_cell) generated by Emont *et al.* ⁴³. *CD300LG*
265 mRNA in ScWAT was primarily expressed in venular endothelial cells, but not adipocytes or
266 other cell types present in ScWAT (Figure 6 B-E).

267



268
 269 **Figure 6. Tissue and cell specific expression of CD300LG.** (A) mRNA levels of CD300LG in a human tissue panel (see Methods). (B-C) snRNAseq
 270 of human adipose tissue, displaying (B) all detected cell clusters and (C) CD300LG related to the clusters (purple color). (D-E) Similar to B-C, but
 271 showing the (D) vascular cell clusters and (E) the corresponding expression of CD300LG (purple color). FPKM = Fragments per kilobase of
 272 transcript per million mapped reads. Data were obtained from Uhlen et al.⁴² and from Emont et al.⁴³ and can be explored at
 273 https://singlecell.broadinstitute.org/single_cell
 274

275 We next explored whether CD300LG mediates tissue-tissue cross-talk using data from the
276 GD-CAT (Genetically-Derived Correlations Across Tissues) database ⁴⁴, which is a tool for
277 analyzing human gene expression correlations in and across multiple tissues. In men, ScWAT
278 *CD300LG* correlated strongly with ScWAT, SkM and aortic gene expression (Supplementary
279 Figure 2). Consistent with our observations in the MyoGlu exercise intervention study, the
280 top network of gene expression in ScWAT related to ScWAT *CD300LG* mRNA was
281 angiogenesis (Supplementary Figure 2 A). Like ScWAT, SkM *CD300LG* also correlated strongly
282 with ScWAT, SkM and aortic gene expression (Supplementary Figure 2 B). The proteasome
283 complex was the top network of gene expression related to SkM *CD300LG* mRNA
284 (Supplementary Figure 2 B). In contrast, running the same analyses in women did not reveal
285 associations between *CD300LG* and angiogenesis (Supplementary Figure 3 A-B).

286

287 We then evaluated serum CD300LG levels in up to 47,747 samples in the UK biobank (see
288 Methods). Descriptive statistics of the UK biobank cohort are presented in Supplementary
289 Table 5. Serum CD300LG levels were positively associated with several measures of physical
290 activity (all metabolic equivalent tasks, results from the international physical activity
291 questionnaire and meeting the recommended amount of weekly physical activity or not;
292 Table 1). Interestingly, serum CD300LG levels were most strongly related to vigorous activity
293 (Table 1). Furthermore, the associations between serum CD300LG and physical activity were
294 significantly stronger in men than in women (Table 1). Serum CD300LG levels were also
295 positively associated with fat mass and fat free mass, and negatively associated with
296 glucometabolic traits including serum glucose levels, Hb1Ac and the risk of having type 2
297 diabetes (Table 1). These associations were independent of body mass index (BMI).

298

Table 1. Multiple regression analyses between serum CD300LG, and measures of physical activity and glucometabolic traits in the UK biobank.

	Women			Men			Interaction			Description	No. of women	No. of men
	Beta-estimate	SE	P	Beta-estimate	SE	P	Beta-estimate	SE	P			
NPX ~ physical activity												
MET per week all activity	1,0E-06	1,2E-06	0,384	4,5E-06	9,9E-07	<0.001	4,3E-06	1,5E-06	0,005	MET minutes per week	22527	20726
MET minutes walking	-6,0E-07	2,6E-06	0,818	-1,8E-06	2,6E-06	0,478	1,7E-07	3,7E-06	0,962	MET minutes per week	22527	20726
MET minutes moderate activity	-2,5E-06	2,4E-06	0,294	1,9E-07	2,3E-06	0,932	1,9E-06	3,3E-06	0,554	MET minutes per week	22527	20726
MET minutes vigorous activity	1,0E-05	2,8E-06	<0.001	2,2E-05	2,1E-06	<2e-16	1,5E-05	3,5E-06	<0.001	MET minutes per week	22527	20726
Sedentary overall average	0,077	0,053	0,147	0,042	0,054	0,441	-0,100	0,075	0,185	Proportion sedentary activity.	7430	5825
Light overall average	-0,119	0,062	0,053	-0,420	0,071	<0.001	-0,232	0,094	0,013	Proportion light activity.	7430	5825
Moderate/vigorous overall average	0,633	0,171	<0.001	1,357	0,194	<0.001	1,043	0,254	<0.001	Proportion moderate/vigorous activity.	7430	5825
IPAQ activity group	9,6E-03	3,8E-03	0,012	3,1E-02	3,8E-03	<0.001	2,6E-02	5,4E-03	<0.001	IPAQ category	22527	20726
Summed days activity	1,9E-03	5,9E-04	<0.001	3,8E-03	5,7E-04	<0.001	2,7E-03	8,1E-04	<0.001	Days performing walking, moderate and vigorous activity	23199	21138
Summed minutes activity	-1,8E-05	3,0E-05	0,550	6,4E-05	2,7E-05	0,017	9,9E-05	4,0E-05	0,013	Mins performing walking, moderate and vigorous activity	22527	20726
Moderate/vigorous recommendation1	7,5E-03	5,6E-03	0,186	4,8E-02	5,8E-03	< 2e-16	4,6E-02	8,0E-03	<0.001	Yes/No	22527	20726
Moderate/vigorous walking recommendation1	-1,3E-05	7,2E-03	0,999	4,0E-02	7,4E-03	<0.001	4,6E-02	1,0E-02	<0.001	Yes/No	22521	20723
Trait ~ NPX												
Body fat percentage impedance	-0,137	0,051	0,007	-0,552	0,052	<0.001	-0,375	0,073	<0.001	Body fat percentage	28099	23802
Whole body fat mass impedance	0,345	0,049	<0.001	0,023	0,051	0,656	-0,209	0,071	0,003	Fat mass (kg)	28108	23866
Whole body fat free mass impedance	0,450	0,050	<0.001	1,045	0,090	<0.001	0,622	0,101	<0.001	Fat free mass (kg)	28107	23870
Body mass index	-	-	-	-	-	-	-	-	-	kg/m2	24810	21509
Glucose	-0,066	0,016	<0.001	-0,041	0,022	0,062	0,033	0,026	0,202	mmol/L	27271	23294
HbA1c	-0,898	0,078	<0.001	-0,911	0,107	<0.001	-0,010	0,130	0,936	mmol/mol	27323	23292
Triglycerides	-0,399	0,011	<0.001	-0,413	0,017	<0.001	-0,058	0,020	0,004	mmol/L	28387	24332
Type 2 diabetes	-0,012	0,002	<0.001	-0,018	0,004	<0.001	0,000	0,004	0,982	Yes/No.	24802	21483
TyG	-2,189	0,074	<0.001	-2,228	0,120	<0.001	-0,203	0,136	0,138	mmol/L x mmol/L	22527	23841

MET = metabolic equivalent of task. NPX = Normalized protein expression. SE = standard error. IPAQ = International physical activity questionnaire. TyG = triglycerid glucose index on insulin resistance.

Model 1 (NPX ~ physical activity) was a linear regression model of NPX values as a function of a measure of physical activity.

Model 2 (Trait ~ NPX) the measures of body composition and glucometabolic traits were the outcomes and NPX values were set as the exposure.

Models 1 and 2 were adjusted for age, batch, study centre, storage time and BMI.

¹Indicates whether a person met the 2017 UK Physical activity guidelines of 150 minutes of moderate activity per week or 75 minutes of vigorous activity.

309 **GWAS of serum CD300LG levels**

310 GWAS analyses of CD300LG levels detected 43 independent genome-wide significant genetic
311 associations across the genome (Supplementary Figure 4). The genomic inflation factor
312 ($\lambda=1.0966$) and LD score intercept (1.039) were consistent with our GWAS being well
313 controlled for population stratification and other possible biases (Supplementary Figure 5).
314 The most significant SNPs lay along chromosome 17 with these SNPs mapping to the
315 genomic region encoding the *CD300LG* gene (Supplementary Figure 4). Follow-up analyses
316 revealed three significant, independent *cis*-pQTLs associated with the protein CD300LG
317 (Supplementary Table 6) and a number of *trans*-pQTLs (Supplementary Table 7).

318

319 *Mendelian randomization (MR) analysis*

320 The independent genome-wide significant SNPs from the CD300LG GWAS were used for
321 two-sample MR (see Methods for details), where 39 SNPs were also available in the
322 outcome GWAS⁴⁵. We first performed Inverse Variance Weighted (IVW) MR analysis to test
323 the causal relationship between CD300LG and fasting glucose, 2-hour post oral glucose
324 tolerance test (OGTT) glucose levels and HbA1c using only *cis*-SNPs (Supplementary Table 8)
325 and all SNPs (Supplementary Table 9). The *cis* IVW MR analysis showed some evidence for a
326 negative causal effect of CD300LG on fasting insulin ($p=0.01$), but due to only three SNPs in
327 these analyses, we could not perform additional sensitivity analyses (except for tests of
328 heterogeneity in estimates of the causal effect across SNPs) and could not determine
329 whether the absence of strong evidence for a causal effect on the glycaemic parameters was
330 genuine or whether our analyses just lacked power. Although some of the analyses involving
331 all the genome-wide significant SNPs indicated a potential causal link between increased
332 serum CD300LG concentration and these outcomes (Supplementary Table 9) the analysis
333 showed significant heterogeneity. We did not detect strong evidence of directional
334 pleiotropy (significant MR Egger intercept, Supplementary Table 9). The heterogeneity in the
335 analysis is possibly due to the fact that many of the SNPs found in the GWAS of CD300LG are
336 associated with related phenotypes which could exert pleiotropic effects on diabetes related
337 outcomes, and so the results should be interpreted with care (Supplementary Table 10). Due
338 to the heterogeneity in our results we therefore performed MR PRESSO to account for
339 outliers. The MR PRESSO analysis showed a significant negative effect of CD300LG on all
340 outcomes (Table 2).

341

342 **Table 2.** Mendelian randomization of serum CD300LG levels and glucose outcomes
343 using MR PRESSO.

Outcome	MR analysis	Number of outliers	Effect	SD	p-value
2-hour post OGTT glucose (mmol/L)	Raw		-0.3722	0.0998	6.2x10 ⁻⁴
2-hour post OGTT glucose (mmol/L)	Outlier-corrected	2	-0.3049	0.0855	1.04x10 ⁻²
Fasting glucose (mmol/L)	Raw		-0.0307	0.0358	0.3963
Fasting glucose (mmol/L)	Outlier-corrected	2	-0.0556	0.0133	1.73x10 ⁻⁴
Fasting insulin (pmol/L)	Raw		-0.0870	0.0558	0.1271
Fasting insulin (pmol/L)	Outlier-corrected	10	-0.0534	0.0252	0.0432
HbA1c (%)	Raw		-0.0485	0.0155	3.28x10 ⁻³
HbA1c (%)	Outlier-corrected	3	-0.0560	0.0155	1.04x10 ⁻⁴

344 For detailed results see Supplementary Table 8 and 9. Fasting glucose adjusted for BMI
345 n=200622, 2-hour post oral glucose tolerance test (OGTT) glucose adjusted for BMI n=63396,
346 fasting insulin adjusted for BMI n=151013, and HbA1c n=146806.

347

348 *Mouse models*

349 To functionally validate association of CD300LG with metabolic homeostasis, we leveraged
350 phenotypic data for exercising mice and for *Cd300lg* deficient (*Cd300lg*^{-/-}) mice that both
351 were publicly available through the MoTrPAC⁴⁶ study and the international mouse
352 phenotyping consortium (PhenoMouse)⁴⁷.

353

354 There is a 51% homology between human *CD300LG* and mouse *Cd300lg*⁴⁸, and also in mice,
355 *Cd300lg* is predominantly expressed in adipose tissue endothelial cells⁴³.

356

357 In MoTrPAC⁴⁶, *Cd300lg* levels in scWAT from n=12-15 male and female mice were increased
358 after exercise for 8 weeks (~30% in both female (p=0.03) and male (p=0.01) mice)
359 (Supplementary Figure 5 A-C). Based on data from n=3050 mice from PhenoMouse male,
360 but not female, mutants for the *Cd300lg*^{tm1a(KOMP)Wtsi} allele displayed impaired glucose
361 tolerance (Supplementary Figure 5 D), but no change in fasting glucose and insulin
362 (Supplementary Figure 5 E-F). Mutant male, but not female, mice also displayed increased
363 lean mass (Supplementary Figure 5 G) and less fat mass (Supplementary Figure 5 H).
364 Detailed PhenoMouse results are presented in Supplementary Table 11.

365

366 Discussion

367 In the present study, we characterized the effects of strength and endurance exercise on the
368 serum proteome of sedentary normal weight and overweight men. We identified significant
369 changes in 283 serum proteins related to many signaling pathways after the 12-week
370 intervention. Some of these proteins were related to the mitochondria, muscle
371 differentiation and exercise capacity. Among known secretory proteins, 19.7% and 12.1%
372 displayed corresponding mRNA changes in SkM and ScWAT, respectively. Although some
373 proteins may be myokines, others may be adipokines or other types of exerkinines. A multi-
374 tissue responding protein was CD300LG, which also correlated positively to insulin
375 sensitivity. CD300LG was particularly interesting because we could replicate the finding in an
376 external cohort, find evidence of a causal link to glucose homeostasis, and perform
377 functionally validation in mice models. Furthermore, the association between CD300LG,
378 physical activity and glycemic traits might display sex dimorphic relationships.

379

380 One of the protein signatures observed in response to exercise was based on strong
381 associations with markers of liver fat content in overweight men. This was related to
382 SLC22A1, which regulates the hepatic glucose-fatty acid cycle affecting gluconeogenesis and
383 lipid metabolism⁴⁹, and may influence liver fat accumulation⁵⁰. This signature also shared
384 many common proteins with a known serum NAFLD proteomic signature³⁸. However, we
385 did not detect overlaps between proteins in this signature and specific gene expression
386 patterns of liver cells (e.g. hepatocytes, immune cells etc.)³⁹. This observation suggests that
387 the proteins detected do not relate to liver protein synthesis per se, but may accumulate in
388 serum due to being released in the blood stream as a result of impaired liver protein
389 catabolism or cell damage as a consequence of overweight/obesity. Notably, this protein
390 signature in overweight men normalized after 12 weeks of exercise and resembled the
391 signature observed in normal weight men. These data suggest -prolonged exercise leads to
392 improvements of liver function in overweight men.

393

394 Several proteins responding to prolonged exercise had a known signal sequence. These
395 secretory proteins are of particular interest because they could mediate inter-tissue
396 adaptations to exercise. For example, COL1A1 was substantially increased in serum and its
397 corresponding mRNA level was increased in SkM. However, COL1A1 is a collagen peptide

398 that is related to muscle damage, turn-over and extracellular matrix remodeling in response
399 to exercise⁵¹ and may mostly reflect muscle restructuring and not represent signaling effects
400 to distant tissues. The large overlap between serum proteins and SkM mRNA most likely
401 suggests a similar phenomenon, where tissue restructuring following exercise is reflected in
402 blood. However, there are probably also several myokines with distant signaling effects
403 among the identified proteins. CCL3 was reduced in serum in parallel with a reduction in its
404 mRNA level in ScWAT. CCL3 is a monocyte chemoattractant protein that may be related to
405 immune cell infiltration in adipose tissue⁵². Hence, this may reflect a positive effect of
406 prolonged exercise on adipose tissue inflammation, which is in line with our previous results
407 showing normalization of adipose tissue inflammation following prolonged exercise¹⁰.

408
409 A particularly interesting protein was CD300LG, which responded to prolonged exercise in
410 serum, and, judged by its mRNA levels, in SkM and ScWAT. Serum CD300LG levels were
411 lower in overweight compared to normal weight men. Furthermore, the exercise-induced
412 response in CD300LG correlated positively to improvements in insulin sensitivity, and there
413 was also a significant correlation between serum CD300LG and insulin sensitivity both
414 before and after the intervention. We therefore analyzed CD300LG in an external data set,
415 the UK Biobank, and again we observed positive associations between especially vigorous
416 exercise and serum CD300LG. Moreover, serum CD300LG levels were negatively associated
417 with glucose levels and type 2 diabetes in the UK Biobank, and these associations might be
418 causal based on MR analysis. These findings were functionally corroborated by the
419 alterations in glucose tolerance and parameters related to insulin sensitivity observed in
420 *Cd300lg*^{-/-} mice. Thus, CD300LG may represent an exerkin with a causal link to glucose
421 homeostasis. However, whether CD300LG can mediate tissue-tissue crosstalk is unknown.
422 CD300LG is a cell surface protein with a transmembrane domain, but is also a predicted
423 secretory protein⁵³. Whether the protein is released from the cell surface in a regulated
424 manner to mediate cross-tissue signaling needs further investigation. Furthermore, the exact
425 link between CD300LG and glucose metabolism is not clear, but possibly related to the fact
426 that CD300LG is expressed in endothelial cells⁵⁴, linked to blood pressure⁵⁵, lymphocyte
427 binding⁵⁶, blood triacylglycerol levels^{57,58} and molecular traffic across the capillary
428 endothelium⁵⁹. Both MyoGlu and GD-CAT data also suggested that CD300LG may be related
429 to angiogenesis in ScWAT⁶⁰ and SkM^{60,61}, at least in men. Hence, we speculate that the link

430 between CD300LG and glucose metabolism is related to improved tissue
431 capillarization/vascular function following prolonged exercise. Furthermore, since vigorous
432 exercise leads to angiogenesis in ScWAT and SkM⁶⁰, serum CD300LG may be a maker of
433 exercise intensity.

434

435 *Limitations and strengths*

436 Although MyoGlu included only 26 sedentary men, they were extensively phenotyped with
437 euglycemic hyperinsulinemic clamp, fitness tests, whole body imaging (MRI/MRS) and
438 mRNA sequencing of ScWAT and SkM. We also supplied our study with data from 47747
439 persons in the UK biobank to enhance the validity and generalization of the results.
440 Furthermore, to assess sex differences we stratified analyses for men and women in the UK
441 Biobank, in external data bases (GD-CAT) and analyzed data from both male and female
442 mice. Since correlations with the clamp data only imply a role for a protein with regard to
443 glucose homeostasis, so we also tested associations with related glucometabolic traits in the
444 UK Biobank and tested these associations for causality using MR. We also included data from
445 exercised mice, and mutant mice to further strengthen the results. Our serum proteome
446 study assessed 3072 proteins, and therefore we do not cover the complete human
447 proteome. However, the Olink platform is based on dual recognition of correctly matched
448 DNA-labeled antibodies, and DNA sequence-specific protein-to-DNA conversion to generate
449 a signal. This is a highly scalable method with an exceptional specificity
450 (<https://olink.com/application/pea/>). Previous exercise-proteomic studies has looked at
451 ~600 proteins in overweight men after endurance exercise²⁵, and three papers were
452 published from the HERITAGE study analyzing ~5000 proteins in response to endurance
453 exercise²⁶⁻²⁸. However, our study is the first and largest exercise study using PEA in both
454 overweight and normal weight men, and also including strength exercise.

455

456 *Conclusion*

457 Our study provided a detailed analysis of serum proteins responding to three months of
458 strength and endurance exercise in both normal weight and overweight men. Our results
459 identified a novel NAFLD-related serum protein signature in overweight men that was
460 normalized after prolonged exercise. We also identified hundreds of tissue-specific and
461 multi-tissue serum markers of e.g., mitochondrial function, muscle differentiation, exercise

462 capacity and insulin sensitivity. Our results were enriched for secretory proteins (exerkines),
463 such as CD300LG, which may be a marker of exercise intensity especially in men, and may
464 also have causal roles in improved glucose homeostasis after physical activity.

465

466 **Methods**

467 The MyoGlu study was conducted as a controlled clinical trial (clinicaltrials.gov:
468 NCT01803568) and was carried out in adherence to the principles of the Declaration of
469 Helsinki. The study received ethical approval from the National Regional Committee for
470 Medical and Health Research Ethics North in Tromsø, Norway, with the reference number
471 2011/882. All participants provided written informed consent before undergoing any
472 procedures related to the study. The UK biobank has ethical approval from the North West
473 Multi-Centre Research Ethics Committee (MREC), which covers the UK, and all participants
474 provided written informed consent. This particular project from the UK biobank received
475 ethical approval from the Institutional Human Research Ethics committee, University of
476 Queensland (approval number 2019002705).

477

478 *Participants*

479 The MyoGlu study enrolled men aged 40 to 65 years who were healthy but sedentary
480 (having engaged in fewer than one exercise session per week in the previous year)^{29,62}.
481 These participants were divided into two groups based on their BMI and glucose tolerance:
482 overweight (with an average BMI of $29.5 \pm 2.3 \text{ kg/m}^2$) and normal weight controls (with an
483 average BMI of $23.6 \pm 2.0 \text{ kg/m}^2$). The overweight men had reduced glucose tolerance
484 and/or insulin sensitivity (Supplementary Table 1). Both groups, consisting of 13 individuals
485 each, underwent a 12-week regimen of combined strength and endurance training.

486

487 *Exercise protocols*

488 This 12-week training intervention included two weekly sessions of 60 minutes each for
489 endurance cycling and two sessions of 60 minutes each for whole-body strength training.
490 Prior to and after the 12-week exercise intervention, a 45-minute bicycle test at 70% of their
491 maximum oxygen uptake (VO_2max) was conducted. Muscle (*m. vastus lateralis*) and
492 subcutaneous white adipose tissue biopsies were taken 48 hours after the last exercise
493 session, both before and after the 12-week intervention period^{29,62}.

494

495 *Clinical data*

496 The euglycaemic hyperinsulinemic clamp was performed after an overnight fast^{29,62}. A fixed
497 dose of insulin 40 mU/m²·min⁻¹ was infused, and glucose (200 mg/mL) was infused to
498 maintain euglycaemia (5.0 mmol/L) for 150 min. Insulin sensitivity is reported as glucose
499 infusion rate (GIR) during the last 30 min relative to body weight. Whole blood glucose
500 concentration was measured using a glucose oxidase method (YSI 2300, Yellow Springs, OH)
501 and plasma glucose concentration was calculated as whole blood glucose x 1.119. Magnetic
502 resonance imaging/spectroscopy (MRI/MRS) methods were used to quantify fat and lean
503 mass. The ankle-to-neck MRI protocol included a 3D DIXON acquisition providing water and
504 lipid quantification, data were then analysed using the nordicICE software package
505 (NordicNeuroLab, Bergen, Norway), and the jMRUI workflow. VO₂max tests were performed
506 after standardized warm-up at a workload similar to the final load of an incremental test in
507 which the relationship between workload (watt) and oxygen uptake was established.
508 Participants cycled for one min followed by a 15 watt increased workload every 30 s until
509 exhaustion. Test success was based on O₂ consumption increased <0.5 mL·kg⁻¹·min⁻¹ over a
510 30 watt increase in workload, respiratory exchange ratio values >1.10, and blood
511 lactate >7.0 mmol/L. We obtained scWAT, SkM biopsies and blood samples as described
512 previously²⁹. Biopsies were obtained from the periumbilical subcutaneous tissue and from
513 *m. vastus lateralis*. After sterilization, a lidocaine based local anaesthetic was injected in the
514 skin and sub cutis prior to both SkM and scWAT biopsies. Biopsies were dissected on a cold
515 aluminium plate to remove blood etc. before freezing. For standard serum parameters,
516 measurement were either conducted using standard in-house methods or outsourced to a
517 commercial laboratory (Fürst Laboratories, Oslo, Norway).

518

519 *The Olink proteomics explorer 3072 platform*

520 We utilized antibody-based technology (Olink Proteomics AB, Uppsala, Sweden) to conduct
521 profiling of serum samples through the Olink Explore 3072 panel. This PEA technique
522 involves using pairs of DNA oligonucleotide-labeled antibodies to bind to the proteins of
523 interest. When two matching antibodies attach to a target protein, the linked
524 oligonucleotides hybridize and are extended by DNA polymerase, forming a unique DNA
525 “barcode”. This barcode is then read using next-generation sequencing. The specificity and

526 sensitivity of the PEA technology are notably high because only accurately matched DNA
527 pairs generated detectable and measurable signals. To refine the dataset, proteins that were
528 not detected or were duplicated were removed, resulting in an analysis of 2886 proteins.
529 Only a single assay was conducted, eliminating inter-assay variability. Data are presented as
530 normalized protein expression (NPX) units, which are logarithmically scaled using a \log_2
531 transformation.

532

533 *Proteomics validations*

534 Duplicate measurements of IL6 and leptin in plasma were conducted using ELISA kits (Leptin;
535 Camarillo, CA and IL6; R&D Systems, Minneapolis, MN) following the manufacturer's
536 instructions. The correlations between PEA or enzyme linked immunosorbent (ELISA) assays
537 were $r=0.94$ ($p=1.4 \times 10^{-11}$), and $r=0.92$ ($p=2.2 \times 10^{-11}$) for IL6 and leptin, respectively
538 (Supplementary Figure 1).

539

540 *mRNA sequencing*

541 Biopsies were frozen in liquid nitrogen, crushed to powder by a pestle in a liquid nitrogen-
542 cooled mortar, transferred into 1 mL QIAzol Lysis Reagent (Qiagen, Hilden, Germany), and
543 homogenized using TissueRuptor (Qiagen) at full speed for 15 sec, twice^{29,62}. Total RNA was
544 isolated from the homogenate using miRNeasy Mini Kit (Qiagen). RNA integrity and
545 concentration were determined using Agilent RNA 6000 Nano Chips on a Bioanalyzer 2100
546 (Agilent Technologies Inc., Santa Clara, CA). RNA was converted to cDNA using High-Capacity
547 cDNA Reverse Transcription Kit (Applied Biosystems, Foster, CA). The cDNA reaction mixture
548 was diluted in water and cDNA equivalent of 25 ng RNA used for each sample. All muscle
549 and scWAT samples were deep-sequenced using the Illumina HiSeq 2000 system with
550 multiplex at the Norwegian Sequencing Centre, University of Oslo. Illumina HiSeq RTA (real-
551 time analysis) v1.17.21.3 was used. Reads passing Illumina's recommended parameters were
552 demultiplexed using CASAVA v1.8.2. For prealignment quality checks, we used the software
553 FastQC v0.10.1. The mean library size was ~44 millions unstranded 51 bp single-ended reads
554 for muscle tissue and ~52 millions for scWAT with no differences between groups or time
555 points. No batch effects were present. cDNA sequenced reads alignment was done using
556 Tophat v2.0.8, Samtools v0.1.18, and Bowtie v2.1.0 with default settings against the UCSC
557 hg19 annotated transcriptome and genome dated 14th of May 2013. Post-alignment quality

558 controls were performed using the Integrative Genome Viewer v2.3 and BED tools v2.19.1.
559 Reads were counted using the intersection strict mode in HTSeq v0.6.1.

560

561 *Statistics and bioinformatics*

562 Olink data were analyzed using the ‘AnalyzeOlink’ R package for pre-processing, testing using
563 mixed linear regression and annotation. Pathway and gene ontology overrepresentation
564 analyses were performed using MSigDB data sets (Hallmark pathways and biological
565 processes). mRNA sequencing data were normalized as reads per kilobase per million
566 mapped read (RPKM) and analyzed using mixed linear regression from the ‘lme4’ R package.
567 Normality was determined by quantile-quantile plots. P-values were corrected using the
568 Benjamini-Hochberg approach set at a false discovery rate (FDR) of 5%. For univariate
569 correlations, Pearsons’ or Spearman’s method were applied as appropriate. Principal
570 component analysis was performed using the ‘prcomp’ R package. Key driver analysis was
571 performed using the ‘Mergeomics’ R package. Mediation analysis was performed using the
572 ‘Mediation’ R package with 1000 bootstraps and the *set.seed* function to ensure
573 reproducibility.

574

575 *UK Biobank*

576 The UK biobank is a large prospective population-based cohort containing ~500,000
577 individuals (~273,000 women), with a variety of phenotypic and genome-wide genetic data
578 available⁶³. The UK biobank has ethical approval from the North West Multi-Centre
579 Research Ethics Committee (MREC), which covers the UK, and all participants provided
580 written informed consent.

581

582 We utilized imputed genetic data from the October 2019 (version 3) release of the UK
583 biobank for our analyses (Application ID: 53641). In addition to the quality control metrics
584 performed centrally by the UK biobank⁶⁴, we defined a subset of unrelated “white
585 European” individuals. We excluded those with putative sex chromosome aneuploidy, high
586 heterozygosity or missing rate, or a mismatch between submitted and inferred sex as
587 identified by the UK biobank (total N = 1932). We excluded individuals who we did not
588 identify as ancestrally European using K-means clustering applied to the first four genetic

589 principal components generated from the 1000 Genomes Project ⁶⁵. We also excluded
590 individuals who had withdrawn their consent to participate in the study as of February 2021.

591

592 The Olink proteomics explorer 1536 platform

593 All analysis were done using the UK Biobank Olink data containing a total of 58699 samples
594 and 54309 individuals, after excluding individuals as mentioned above we had 47747
595 samples with measured serum CD300LG levels. Data was generated according to Olink's
596 standard procedures.

597

598 Observational analyses

599 For the physical activity measurements we investigated if the degree of physical activity was
600 associated with serum levels of protein (serum levels of protein regressed on physical
601 activity), alternatively for the metabolic measurements we investigated if the protein
602 expression affected the metabolic measurements (trait regressed on serum levels of
603 protein), for both we used a linear regression model. We performed analyses stratified by
604 sex and adjusting for age, protein batch, UK Biobank assessment centre, the time the sample
605 was stored and BMI. All analyses were performed in R version 3.4.3.

606

607 Genome-wide association analysis

608 A GWAS of serum CD300LG levels (\log_2 transformed) measured in the UK Biobank was
609 performed using BOLT-LMM ⁶⁶ on individuals of European descent who had proteomic data
610 available (N=45788). We included sex, year of birth, protein and genotyping batch, time
611 from sample collection to processing time (in weeks) and five ancestry informative principal
612 components as covariates in the analysis.

613

614 Post GWAS quality control included the removal of SNPs with $MAF \leq 0.05$ and info score ≤ 0.4
615 ($n_{SNPs}=6,945,819$). The previously generated LD reference panel for clumping consisted of a
616 random sample of 47674 unrelated British UK biobank individuals identified using GCTA ⁶⁷
617 with identity by state (IBS) <0.025 and identity by descent (IBD) sharing of <0.1 . LD score
618 regression analysis ⁶⁸ was used to investigate whether genomic inflation was likely due to
619 polygenicity or population stratification/cryptic relatedness.

620

621 Prior to gene annotation palindromic SNPs were excluded ($n_{\text{SNPs}}=6,882,889$ remaining).
622 Variants were classified as either *cis*- or *trans*-pQTLs based on SNP proximity to the protein-
623 encoding gene (CD300LG) of interest. Variant annotation was performed using ANNOVAR⁶⁹,
624 labelling genes +/-500kb from variants. A pQTL was considered a *cis*-pQTL if the gene
625 annotation in the 1Mb window matched the protein name, all remaining variants were
626 considered *trans*-pQTLs.

627
628 To extract independent genome-wide significant pQTLs ($p < 5 \times 10^{-8}$) clumping was performed
629 using the PLINK v1.90b3.31 software package⁷⁰; variants with $r^2 > 0.001$ with the index SNP
630 were removed using a 1 Mb window. Variants which lied within the human major
631 histocompatibility complex (MHC) region were removed, excluding pQTLs on chromosome 6
632 from 26Mb to 34Mb.

633
634 *Mendelian Randomization (MR)*

635 To obtain valid instrumental variables (SNPs) for our analysis we assessed them against the
636 three core assumptions for MR analysis: 1) That the SNPs were robustly associated with the
637 exposure of interest. For that we obtained summary result statistics on genome-wide
638 significant SNPs from our own GWAS. 2) That the SNPs were not associated with any known
639 or unknown confounders. This is not an assumption that can be fully tested, however we
640 used PhenoScanner^{71,72} to assess whether any SNPs were associated with known
641 confounders (described below). 3) That the SNPs were not associated with the outcomes
642 through any other path than through the exposure. To test this assumption, we searched
643 PhenoScanner^{71,72} (detailed below) to see if our exposures of interest were associated with
644 other potentially pleiotropic phenotypes.

645
646 MR statistical analysis

647 We used the TwoSampleMR package⁷³ (<https://github.com/MRCIEU/TwoSampleMR>) in R
648 version 4.2.2 (<https://cran.r-project.org/>). The outcome studies were obtained from
649 <https://www.magicinvestigators.org/>⁴⁵ and were external to the UK biobank. Specifically,
650 we used the outcomes "fasting glucose adjusted for BMI" (mmol/L, n=200622), "2-hour post
651 OGTT glucose adjusted for BMI" (mmol/L, n=63396), "fasting insulin adjusted for BMI"
652 (pmol/L, n=151013) and "HbA1c" (% , n=146806)⁴⁵.

653

654 We performed a two-sample inverse variance weighted (IVW) analysis to assess the causal
655 effect of CD300LG on metabolic factors (Supplementary Table 8 and 9). To explore potential
656 violations of the core assumptions when using the full set of SNPs, we performed a
657 heterogeneity test using Cochran's Q, and a test for directional pleiotropy was conducted by
658 assessing the degree to which the MR Egger intercept differed from zero ⁷⁴. We also
659 performed additional sensitivity analyses using MR Egger regression ⁷⁴, weighted median ⁷⁵,
660 simple and weighted mode estimation methods ⁷⁶. Effect estimates from the different
661 sensitivity analysis were compared as a way of assessing the robustness of the results. To
662 assess potential heterogeneity in the MR estimates we further performed MR-PRESSO ^{45,77}
663 to detect (MR-PRESSO global test) and correct for horizontal pleiotropy via outlier removal
664 (MR-PRESSO outlier test).

665

666 Investigation of potentially pleiotropic SNPs

667 SNPs robustly associated with the exposure investigated in the MR analyses (serum CD300LG
668 levels) were checked for other possible associations (PhenoScanner v2 ^{71,72},
669 <http://www.phenoscanter.medschl.cam.ac.uk/>) which may contribute to a pleiotropic effect
670 on the metabolic outcomes. Supplementary Table 10 lists the SNPs used in our analysis that
671 many influence related phenotypes. Phenotypes from PhenoScanner were listed if they
672 were associated with the SNPs or nearby variants in high LD ($r^2=0.8$) at p-value level $<1 \times 10^{-5}$
673 and could have potential pleiotropic effects in the analysis.

674

675 *Data availability*

676 mRNA sequencing data from MyoGlu can be found at
677 <https://exchmdpmsg.medsch.ucla.edu/app/> as well as in GEO:GSE227419. Secretory proteins
678 are available in the MetazSeckB data base at
679 <http://proteomics.yyu.edu/secretomes/animal/>. The human serum proteomic NAFLD
680 signature is available in the study of Govaere *et al* ³⁸. Expression profiles in human liver cells
681 are available in the Human Liver Cell Atlas ³⁹. Data obtained from the UK biobank (Olink
682 explore 1536 and measures of physical activity ⁷⁸ can be found at
683 <https://biobank.ndph.ox.ac.uk/ukb/>. Glucometabolic outcomes used in MR analyses are
684 available at: <https://www.magicinvestigators.org/> ⁴⁵. Data from the GD-CAT database is

685 available from: <https://pipeline.biochem.uci.edu/gtex/demo2/>. Mice exercise data are
686 available at <https://motrpcac-data.org/> and knock-out data at
687 <https://www.mousephenotype.org/>. CD300LG expression values from a human tissue panel
688 were obtained from Uhlén *et al.*⁴². The single nuclei mRNA sequencing data from human
689 adipose tissue was plotted in Seurat v. 4 by downloading processed data from the Single Cell
690 Portal⁴³. The data can also be explored at:
691 [https://singlecell.broadinstitute.org/single_cell/study/SCP1376/a-single-cell-atlas-of-human-](https://singlecell.broadinstitute.org/single_cell/study/SCP1376/a-single-cell-atlas-of-human-and-mouse-white-adipose-tissue)
692 [and-mouse-white-adipose-tissue](https://singlecell.broadinstitute.org/single_cell/study/SCP1376/a-single-cell-atlas-of-human-and-mouse-white-adipose-tissue)). UK Biobank (<https://www.ukbiobank.ac.uk/>) data are
693 available to researchers upon application to the individual cohorts via their websites. All
694 other data used are publicly available and referenced according in the main text. For
695 additional details and data inquiries, please contact Sindre Lee-Ødegård.

696

697 **Acknowledgements**

698 South-Eastern Norway Regional Health Authority, Simon Fougner's fund, Diabetesforbundet,
699 Johan Selmer Kvanes' legat til forskning og bekjempelse av sukkersyke. This research has
700 been conducted using the UK Biobank resource (Reference 53641). DME is funded by an
701 Australian National Health and Medical Research Council Investigator Grant (APP2017942).
702 GHM is the recipient of an Australian Research Council Discovery Early Career Award
703 (Project number: DE220101226) funded by the Australian Government and supported by
704 the Research Council of Norway (Project grant: 325640 & Mobility grant: 287198).

705

706 **Author contributions**

707 Conceptualization: SLØ, CAD, KIB. Methodology: SLØ, GHM, ED, DME. Data Collection: SLØ,
708 FN. Data analysis: SLØ, TO, MH, GHM, ED. Visualization: SLØ, GHM and MH. Writing original
709 draft: SLØ. Writing, review and editing: SLØ, MH, TO, GHM, ED, DME, JKV, HLG, FN, CAD, KIB.
710 Supervision: CAD, KIB. Funding acquisition : SLØ, CAD, KIB. Project administration: KIB.

711

712 **Competing interests**

713 The authors declare no conflict of interest.

714

715 **References**

- 716 1. Piercy, K.L., Troiano, R.P., Ballard, R.M., Carlson, S.A., Fulton, J.E., Galuska, D.A.,
717 George, S.M., and Olson, R.D. (2018). The Physical Activity Guidelines for Americans.
718 *Jama* 320, 2020-2028. 10.1001/jama.2018.14854.
- 719 2. Hawley, J.A., and Lessard, S.J. (2008). Exercise training-induced improvements in
720 insulin action. *Acta Physiol (Oxf)* 192, 127-135. 10.1111/j.1748-1716.2007.01783.x.
- 721 3. Bacchi, E., Negri, C., Zanolin, M.E., Milanese, C., Faccioli, N., Trombetta, M., Zoppini,
722 G., Cevese, A., Bonadonna, R.C., Schena, F., et al. (2012). Metabolic effects of aerobic
723 training and resistance training in type 2 diabetic subjects: a randomized controlled
724 trial (the RAED2 study). *Diabetes care* 35, 676-682. 10.2337/dc11-1655.
- 725 4. Pedersen, B.K., Akerström, T.C., Nielsen, A.R., and Fischer, C.P. (2007). Role of
726 myokines in exercise and metabolism. *Journal of applied physiology (Bethesda, Md. :
727 1985)* 103, 1093-1098. 10.1152/jappphysiol.00080.2007.
- 728 5. Chow, L.S., Gerszten, R.E., Taylor, J.M., Pedersen, B.K., van Praag, H., Trappe, S.,
729 Febbraio, M.A., Galis, Z.S., Gao, Y., Haus, J.M., et al. (2022). Exerkines in health,
730 resilience and disease. *Nat Rev Endocrinol* 18, 273-289. 10.1038/s41574-022-00641-
731 2.
- 732 6. Görgens, S.W., Eckardt, K., Jensen, J., Drevon, C.A., and Eckel, J. (2015). Exercise and
733 Regulation of Adipokine and Myokine Production. *Progress in molecular biology and
734 translational science* 135, 313-336. 10.1016/bs.pmbts.2015.07.002.
- 735 7. Lee-Ødegård, S., Olsen, T., Norheim, F., Drevon, C.A., and Birkeland, K.I. (2022).
736 Potential Mechanisms for How Long-Term Physical Activity May Reduce Insulin
737 Resistance. *Metabolites* 12. 10.3390/metabo12030208.
- 738 8. Pourteymour, S., Eckardt, K., Holen, T., Langleite, T., Lee, S., Jensen, J., Birkeland, K.I.,
739 Drevon, C.A., and Hjorth, M. (2017). Global mRNA sequencing of human skeletal
740 muscle: Search for novel exercise-regulated myokines. *Molecular metabolism* 6, 352-
741 365. 10.1016/j.molmet.2017.01.007.
- 742 9. Pedersen, B.K., and Febbraio, M.A. (2012). Muscles, exercise and obesity: skeletal
743 muscle as a secretory organ. *Nat Rev Endocrinol* 8, 457-465.
744 10.1038/nrendo.2012.49.
- 745 10. Lee, S., Norheim, F., Langleite, T.M., Gulseth, H.L., Birkeland, K.I., and Drevon, C.A.
746 (2019). Effects of long-term exercise on plasma adipokine levels and inflammation-
747 related gene expression in subcutaneous adipose tissue in sedentary dysglycaemic,
748 overweight men and sedentary normoglycaemic men of healthy weight. *Diabetologia*
749 62, 1048-1064. 10.1007/s00125-019-4866-5.
- 750 11. Bouassida, A., Chamari, K., Zaouali, M., Feki, Y., Zbidi, A., and Tabka, Z. (2010). Review
751 on leptin and adiponectin responses and adaptations to acute and chronic exercise.
752 *Br J Sports Med* 44, 620-630. 10.1136/bjism.2008.046151.
- 753 12. Stanford, K.I., Lynes, M.D., Takahashi, H., Baer, L.A., Arts, P.J., May, F.J., Lehnig, A.C.,
754 Middelbeek, R.J.W., Richard, J.J., So, K., et al. (2018). 12,13-diHOME: An Exercise-
755 Induced Lipokine that Increases Skeletal Muscle Fatty Acid Uptake. *Cell metabolism*
756 27, 1111-1120.e1113. 10.1016/j.cmet.2018.03.020.
- 757 13. Lee, S., Norheim, F., Gulseth, H.L., Langleite, T.M., Kolnes, K.J., Tangen, D.S.,
758 Stadheim, H.K., Gilfillan, G.D., Holen, T., Birkeland, K.I., et al. (2017). Interaction
759 between plasma fetuin-A and free fatty acids predicts changes in insulin sensitivity in
760 response to long-term exercise. *Physiological reports* 5. 10.14814/phy2.13183.

- 761 14. Kistner, T.M., Pedersen, B.K., and Lieberman, D.E. (2022). Interleukin 6 as an energy
762 allocator in muscle tissue. *Nature Metabolism* 4, 170-179. [10.1038/s42255-022-](https://doi.org/10.1038/s42255-022-00538-4)
763 [00538-4](https://doi.org/10.1038/s42255-022-00538-4).
- 764 15. Haugen, F., Norheim, F., Lian, H., Wensaas, A.J., Dueland, S., Berg, O., Funderud, A.,
765 Skålhegg, B.S., Raastad, T., and Drevon, C.A. (2010). IL-7 is expressed and secreted by
766 human skeletal muscle cells. *Am J Physiol Cell Physiol* 298, C807-816.
767 [10.1152/ajpcell.00094.2009](https://doi.org/10.1152/ajpcell.00094.2009).
- 768 16. Otaka, N., Shibata, R., Ohashi, K., Uemura, Y., Kambara, T., Enomoto, T., Ogawa, H.,
769 Ito, M., Kawanishi, H., Maruyama, S., et al. (2018). Myonectin Is an Exercise-Induced
770 Myokine That Protects the Heart From Ischemia-Reperfusion Injury. *Circ Res* 123,
771 1326-1338. [10.1161/circresaha.118.313777](https://doi.org/10.1161/circresaha.118.313777).
- 772 17. Hjorth, M., Pourteymour, S., Görgens, S.W., Langleite, T.M., Lee, S., Holen, T., Gulseth,
773 H.L., Birkeland, K.I., Jensen, J., Drevon, C.A., and Norheim, F. (2016). Myostatin in
774 relation to physical activity and dysglycaemia and its effect on energy metabolism in
775 human skeletal muscle cells. *Acta Physiol (Oxf)* 217, 45-60. [10.1111/apha.12631](https://doi.org/10.1111/apha.12631).
- 776 18. McPherron, A.C., Lawler, A.M., and Lee, S.J. (1997). Regulation of skeletal muscle
777 mass in mice by a new TGF-beta superfamily member. *Nature* 387, 83-90.
778 [10.1038/387083a0](https://doi.org/10.1038/387083a0).
- 779 19. Rao, R.R., Long, J.Z., White, J.P., Svensson, K.J., Lou, J., Lokurkar, I., Jedrychowski,
780 M.P., Ruas, J.L., Wrann, C.D., Lo, J.C., et al. (2014). Meteorin-like is a hormone that
781 regulates immune-adipose interactions to increase beige fat thermogenesis. *Cell* 157,
782 1279-1291. [10.1016/j.cell.2014.03.065](https://doi.org/10.1016/j.cell.2014.03.065).
- 783 20. Kanzleiter, T., Rath, M., Gorgens, S.W., Jensen, J., Tangen, D.S., Kolnes, A.J., Kolnes,
784 K.J., Lee, S., Eckel, J., Schurmann, A., and Eckardt, K. (2014). The myokine decorin is
785 regulated by contraction and involved in muscle hypertrophy. *Biochemical and*
786 *biophysical research communications* 450, 1089-1094. [10.1016/j.bbrc.2014.06.123](https://doi.org/10.1016/j.bbrc.2014.06.123).
- 787 21. Malin, S.K., del Rincon, J.P., Huang, H., and Kirwan, J.P. (2014). Exercise-induced
788 lowering of fetuin-A may increase hepatic insulin sensitivity. *Medicine and science in*
789 *sports and exercise* 46, 2085-2090. [10.1249/mss.0000000000000338](https://doi.org/10.1249/mss.0000000000000338).
- 790 22. Catoire, M., Alex, S., Paraskevopoulos, N., Mattijssen, F., Evers-van Gogh, I., Schaart,
791 G., Jeppesen, J., Kneppers, A., Mensink, M., Voshol, P.J., et al. (2014). Fatty acid-
792 inducible ANGPTL4 governs lipid metabolic response to exercise. *Proceedings of the*
793 *National Academy of Sciences of the United States of America* 111, E1043-1052.
794 [10.1073/pnas.1400889111](https://doi.org/10.1073/pnas.1400889111).
- 795 23. Norheim, F., Hjorth, M., Langleite, T.M., Lee, S., Holen, T., Bindesboll, C., Stadheim,
796 H.K., Gulseth, H.L., Birkeland, K.I., Kielland, A., et al. (2014). Regulation of
797 angiopoietin-like protein 4 production during and after exercise. *Physiological reports*
798 2. [10.14814/phy2.12109](https://doi.org/10.14814/phy2.12109).
- 799 24. Contrepolis, K., Wu, S., Moneghetti, K.J., Hornburg, D., Ahadi, S., Tsai, M.S., Metwally,
800 A.A., Wei, E., Lee-McMullen, B., Quijada, J.V., et al. (2020). Molecular Choreography
801 of Acute Exercise. *Cell* 181, 1112-1130.e1116. [10.1016/j.cell.2020.04.043](https://doi.org/10.1016/j.cell.2020.04.043).
- 802 25. Diaz-Canestro, C., Chen, J., Liu, Y., Han, H., Wang, Y., Honoré, E., Lee, C.H., Lam, K.S.L.,
803 Tse, M.A., and Xu, A. (2023). A machine-learning algorithm integrating baseline
804 serum proteomic signatures predicts exercise responsiveness in overweight males
805 with prediabetes. *Cell Rep Med* 4, 100944. [10.1016/j.xcrm.2023.100944](https://doi.org/10.1016/j.xcrm.2023.100944).
- 806 26. Robbins, J.M., Peterson, B., Schraner, D., Tahir, U.A., Rienmüller, T., Deng, S., Keyes,
807 M.J., Katz, D.H., Beltran, P.M.J., Barber, J.L., et al. (2021). Human plasma proteomic

- 808 profiles indicative of cardiorespiratory fitness. *Nat Metab* 3, 786-797.
809 10.1038/s42255-021-00400-z.
- 810 27. Robbins, J.M., Rao, P., Deng, S., Keyes, M.J., Tahir, U.A., Katz, D.H., Beltran, P.M.J.,
811 Marchildon, F., Barber, J.L., Peterson, B., et al. (2023). Plasma proteomic changes in
812 response to exercise training are associated with cardiorespiratory fitness
813 adaptations. *JCI Insight* 8. 10.1172/jci.insight.165867.
- 814 28. Mi, M.Y., Barber, J.L., Rao, P., Farrell, L.A., Sarzynski, M.A., Bouchard, C., Robbins, J.M.,
815 and Gerszten, R.E. (2023). Plasma Proteomic Kinetics in Response to Acute Exercise.
816 *Mol Cell Proteomics* 22, 100601. 10.1016/j.mcpro.2023.100601.
- 817 29. Langleite, T.M., Jensen, J., Norheim, F., Gulseth, H.L., Tangen, D.S., Kolnes, K.J., Heck,
818 A., Storås, T., Grothe, G., Dahl, M.A., et al. (2016). Insulin sensitivity, body
819 composition and adipose depots following 12 w combined endurance and strength
820 training in dysglycemic and normoglycemic sedentary men. *Archives of physiology
821 and biochemistry* 122, 167-179. 10.1080/13813455.2016.1202985.
- 822 30. Sudlow, C., Gallacher, J., Allen, N., Beral, V., Burton, P., Danesh, J., Downey, P., Elliott,
823 P., Green, J., Landray, M., et al. (2015). UK Biobank: An Open Access Resource for
824 Identifying the Causes of a Wide Range of Complex Diseases of Middle and Old Age.
825 *PLOS Medicine* 12, e1001779. 10.1371/journal.pmed.1001779.
- 826 31. Hamaguchi, H., Dohi, K., Sakai, T., Taoka, M., Isobe, T., Matsui, T.S., Deguchi, S.,
827 Furuichi, Y., Fujii, N.L., and Manabe, Y. (2023). PDGF-B secreted from skeletal muscle
828 enhances myoblast proliferation and myotube maturation via activation of the
829 PDGFR signaling cascade. *Biochemical and biophysical research communications* 639,
830 169-175. <https://doi.org/10.1016/j.bbrc.2022.11.085>.
- 831 32. Lories, R.J., Peeters, J., Szlufcik, K., Hespel, P., and Luyten, F.P. (2009). Deletion of
832 frizzled-related protein reduces voluntary running exercise performance in mice.
833 *Osteoarthritis Cartilage* 17, 390-396. 10.1016/j.joca.2008.07.018.
- 834 33. Casas-Fraile, L., Cornelis, F.M., Costamagna, D., Rico, A., Duelen, R., Sampaolesi,
835 M.M., López de Munain, A., Lories, R.J., and Sáenz, A. (2020). Frizzled related protein
836 deficiency impairs muscle strength, gait and calpain 3 levels. *Orphanet Journal of
837 Rare Diseases* 15, 119. 10.1186/s13023-020-01372-1.
- 838 34. López-Bellón, S., Rodríguez-López, S., González-Reyes, J.A., Burón, M.I., de Cabo, R.,
839 and Villalba, J.M. (2022). CYB5R3 overexpression preserves skeletal muscle
840 mitochondria and autophagic signaling in aged transgenic mice. *Geroscience* 44,
841 2223-2241. 10.1007/s11357-022-00574-8.
- 842 35. Tassi, E., Garman, K.A., Schmidt, M.O., Ma, X., Kabbara, K.W., Uren, A., Tomita, Y.,
843 Goetz, R., Mohammadi, M., Wilcox, C.S., et al. (2018). Fibroblast Growth Factor
844 Binding Protein 3 (FGFBP3) impacts carbohydrate and lipid metabolism. *Sci Rep* 8,
845 15973. 10.1038/s41598-018-34238-5.
- 846 36. Qian, Q., Hu, F., Yu, W., Leng, D., Li, Y., Shi, H., Deng, D., Ding, K., Liang, C., and Liu, J.
847 (2023). SWAP70 Overexpression Protects Against Pathological Cardiac Hypertrophy in
848 a TAK1-Dependent Manner. *J Am Heart Assoc* 12, e028628.
849 10.1161/jaha.122.028628.
- 850 37. Chen, H.H., Luche, R., Wei, B., and Tonks, N.K. (2004). Characterization of two distinct
851 dual specificity phosphatases encoded in alternative open reading frames of a single
852 gene located on human chromosome 10q22.2. *The Journal of biological chemistry*
853 279, 41404-41413. 10.1074/jbc.M405286200.

- 854 38. Govaere, O., Hasoon, M., Alexander, L., Cockell, S., Tiniakos, D., Ekstedt, M.,
855 Schattenberg, J.M., Boursier, J., Bugianesi, E., Ratziu, V., et al. (2023). A proteo-
856 transcriptomic map of non-alcoholic fatty liver disease signatures. *Nature*
857 *Metabolism* 5, 572-578. [10.1038/s42255-023-00775-1](https://doi.org/10.1038/s42255-023-00775-1).
- 858 39. Aizarani, N., Saviano, A., Sagar, Mailly, L., Durand, S., Herman, J.S., Pessaux, P.,
859 Baumert, T.F., and Grün, D. (2019). A human liver cell atlas reveals heterogeneity and
860 epithelial progenitors. *Nature* 572, 199-204. [10.1038/s41586-019-1373-2](https://doi.org/10.1038/s41586-019-1373-2).
- 861 40. Montgomery, M.K., Bayliss, J., Devereux, C., Bezawork-Geleta, A., Roberts, D., Huang,
862 C., Schittenhelm, R.B., Ryan, A., Townley, S.L., Selth, L.A., et al. (2020). SMOC1 is a
863 glucose-responsive hepatokine and therapeutic target for glycemic control. *Sci Transl*
864 *Med* 12. [10.1126/scitranslmed.aaz8048](https://doi.org/10.1126/scitranslmed.aaz8048).
- 865 41. Ghodsian, N., Gagnon, E., Bourgault, J., Gobeil, É., Manikpurage, H.D., Perrot, N.,
866 Girard, A., Mitchell, P.L., and Arsenault, B.J. (2021). Blood Levels of the SMOC1
867 Hepatokine Are Not Causally Linked with Type 2 Diabetes: A Bidirectional Mendelian
868 Randomization Study. *Nutrients* 13. [10.3390/nu13124208](https://doi.org/10.3390/nu13124208).
- 869 42. Uhlén, M., Fagerberg, L., Hallström, B.M., Lindskog, C., Oksvold, P., Mardinoglu, A.,
870 Sivertsson, Å., Kampf, C., Sjöstedt, E., Asplund, A., et al. (2015). Proteomics. Tissue-
871 based map of the human proteome. *Science (New York, N.Y.)* 347, 1260419.
872 [10.1126/science.1260419](https://doi.org/10.1126/science.1260419).
- 873 43. Emont, M.P., Jacobs, C., Essene, A.L., Pant, D., Tenen, D., Colleluori, G., Di Vincenzo,
874 A., Jørgensen, A.M., Dashti, H., Stefek, A., et al. (2022). A single-cell atlas of human
875 and mouse white adipose tissue. *Nature* 603, 926-933. [10.1038/s41586-022-04518-2](https://doi.org/10.1038/s41586-022-04518-2).
- 877 44. Battle, A., Brown, C.D., Engelhardt, B.E., and Montgomery, S.B. (2017). Genetic
878 effects on gene expression across human tissues. *Nature* 550, 204-213.
879 [10.1038/nature24277](https://doi.org/10.1038/nature24277).
- 880 45. Chen, J., Spracklen, C.N., Marenne, G., Varshney, A., Corbin, L.J., Luan, J., Willems,
881 S.M., Wu, Y., Zhang, X., Horikoshi, M., et al. (2021). The trans-ancestral genomic
882 architecture of glycemic traits. *Nat Genet* 53, 840-860. [10.1038/s41588-021-00852-9](https://doi.org/10.1038/s41588-021-00852-9).
- 883 46. Sanford, J.A., Nogiec, C.D., Lindholm, M.E., Adkins, J.N., Amar, D., Dasari, S., Drugan,
884 J.K., Fernández, F.M., Radom-Aizik, S., Schenk, S., et al. (2020). Molecular Transducers
885 of Physical Activity Consortium (MoTrPAC): Mapping the Dynamic Responses to
886 Exercise. *Cell* 181, 1464-1474. [10.1016/j.cell.2020.06.004](https://doi.org/10.1016/j.cell.2020.06.004).
- 887 47. Dickinson, M.E., Flenniken, A.M., Ji, X., Teboul, L., Wong, M.D., White, J.K., Meehan,
888 T.F., Weninger, W.J., Westerberg, H., Adissu, H., et al. (2016). High-throughput
889 discovery of novel developmental phenotypes. *Nature* 537, 508-514.
890 [10.1038/nature19356](https://doi.org/10.1038/nature19356).
- 891 48. Takatsu, H., Hase, K., Ohmae, M., Ohshima, S., Hashimoto, K., Taniura, N., Yamamoto,
892 A., and Ohno, H. (2006). CD300 antigen like family member G: A novel Ig receptor like
893 protein exclusively expressed on capillary endothelium. *Biochemical and biophysical*
894 *research communications* 348, 183-191. <https://doi.org/10.1016/j.bbrc.2006.07.047>.
- 895 49. Liang, X., Yee, S.W., Chien, H.C., Chen, E.C., Luo, Q., Zou, L., Piao, M., Mifune, A.,
896 Chen, L., Calvert, M.E., et al. (2018). Organic cation transporter 1 (OCT1) modulates
897 multiple cardiometabolic traits through effects on hepatic thiamine content. *PLoS*
898 *Biol* 16, e2002907. [10.1371/journal.pbio.2002907](https://doi.org/10.1371/journal.pbio.2002907).
- 899 50. Chen, L., Shu, Y., Liang, X., Chen, E.C., Yee, S.W., Zur, A.A., Li, S., Xu, L., Keshari, K.R.,
900 Lin, M.J., et al. (2014). OCT1 is a high-capacity thiamine transporter that regulates

- 901 hepatic steatosis and is a target of metformin. *Proceedings of the National Academy*
902 *of Sciences of the United States of America* *111*, 9983-9988.
903 [10.1073/pnas.1314939111](https://doi.org/10.1073/pnas.1314939111).
- 904 51. Jacob, Y., Anderton, R.S., Cochrane Wilkie, J.L., Rogalski, B., Laws, S.M., Jones, A.,
905 Spiteri, T., Hince, D., and Hart, N.H. (2022). Genetic Variants within NOGGIN, COL1A1,
906 COL5A1, and IGF2 are Associated with Musculoskeletal Injuries in Elite Male
907 Australian Football League Players: A Preliminary Study. *Sports Medicine - Open* *8*,
908 126. [10.1186/s40798-022-00522-y](https://doi.org/10.1186/s40798-022-00522-y).
- 909 52. Barry, J.C., Simtchouk, S., Durrer, C., Jung, M.E., and Little, J.P. (2017). Short-Term
910 Exercise Training Alters Leukocyte Chemokine Receptors in Obese Adults. *Medicine*
911 *and science in sports and exercise* *49*, 1631-1640. [10.1249/mss.0000000000001261](https://doi.org/10.1249/mss.0000000000001261).
- 912 53. Meinken, J., Walker, G., Cooper, C.R., and Min, X.J. (2015). MetazSecKB: the human
913 and animal secretome and subcellular proteome knowledgebase. *Database (Oxford)*
914 *2015*. [10.1093/database/bav077](https://doi.org/10.1093/database/bav077).
- 915 54. Umemoto, E., Takeda, A., Jin, S., Luo, Z., Nakhogi, N., Hayasaka, H., Lee, C.M.,
916 Tanaka, T., and Miyasaka, M. (2013). Dynamic changes in endothelial cell adhesion
917 molecule nepmucin/CD300LG expression under physiological and pathological
918 conditions. *PloS one* *8*, e83681. [10.1371/journal.pone.0083681](https://doi.org/10.1371/journal.pone.0083681).
- 919 55. Støy, J., Grarup, N., Hørlyck, A., Ibsen, L., Rungby, J., Poulsen, P.L., Brandslund, I.,
920 Christensen, C., Hansen, T., Pedersen, O., et al. (2014). Blood pressure levels in male
921 carriers of Arg82Cys in CD300LG. *PloS one* *9*, e109646.
922 [10.1371/journal.pone.0109646](https://doi.org/10.1371/journal.pone.0109646).
- 923 56. Umemoto, E., Tanaka, T., Kanda, H., Jin, S., Tohya, K., Otani, K., Matsutani, T.,
924 Matsumoto, M., Ebisuno, Y., Jang, M.H., et al. (2006). Nepmucin, a novel HEV
925 sialomucin, mediates L-selectin-dependent lymphocyte rolling and promotes
926 lymphocyte adhesion under flow. *J Exp Med* *203*, 1603-1614.
927 [10.1084/jem.20052543](https://doi.org/10.1084/jem.20052543).
- 928 57. Surakka, I., Horikoshi, M., Mägi, R., Sarin, A.-P., Mahajan, A., Lagou, V., Marullo, L.,
929 Ferreira, T., Miraglio, B., Timonen, S., et al. (2015). The impact of low-frequency and
930 rare variants on lipid levels. *Nature Genetics* *47*, 589-597. [10.1038/ng.3300](https://doi.org/10.1038/ng.3300).
- 931 58. Støy, J., Kampmann, U., Mengel, A., Magnusson, N.E., Jessen, N., Grarup, N., Rungby,
932 J., Stødkilde-Jørgensen, H., Brandslund, I., Christensen, C., et al. (2015). Reduced
933 CD300LG mRNA tissue expression, increased intramyocellular lipid content and
934 impaired glucose metabolism in healthy male carriers of Arg82Cys in CD300LG: a
935 novel genometic cross-link between CD300LG and common metabolic
936 phenotypes. *BMJ Open Diabetes Res Care* *3*, e000095. [10.1136/bmjdr-2015-000095](https://doi.org/10.1136/bmjdr-2015-000095).
- 937
- 938 59. Takatsu, H., Hase, K., Ohmae, M., Ohshima, S., Hashimoto, K., Taniura, N., Yamamoto,
939 A., and Ohno, H. (2006). CD300 antigen like family member G: A novel Ig receptor like
940 protein exclusively expressed on capillary endothelium. *Biochemical and biophysical*
941 *research communications* *348*, 183-191. [10.1016/j.bbrc.2006.07.047](https://doi.org/10.1016/j.bbrc.2006.07.047).
- 942 60. Van Pelt, D.W., Guth, L.M., and Horowitz, J.F. (2017). Aerobic exercise elevates
943 markers of angiogenesis and macrophage IL-6 gene expression in the subcutaneous
944 adipose tissue of overweight-to-obese adults. *Journal of applied physiology* *123*,
945 1150-1159. [10.1152/jappphysiol.00614.2017](https://doi.org/10.1152/jappphysiol.00614.2017).
- 946 61. Ross, M., Kargl, C.K., Ferguson, R., Gavin, T.P., and Hellsten, Y. (2023). Exercise-
947 induced skeletal muscle angiogenesis: impact of age, sex, angiocrines and cellular

- 948 mediators. *European Journal of Applied Physiology* 123, 1415-1432. 10.1007/s00421-
949 022-05128-6.
- 950 62. Lee, S., Gulseth, H.L., Langleite, T.M., Norheim, F., Olsen, T., Refsum, H., Jensen, J.,
951 Birkeland, K.I., and Drevon, C.A. (2021). Branched-chain amino acid metabolism,
952 insulin sensitivity and liver fat response to exercise training in sedentary
953 dysglycaemic and normoglycaemic men. *Diabetologia* 64, 410-423. 10.1007/s00125-
954 020-05296-0.
- 955 63. Sudlow, C., Gallacher, J., Allen, N., Beral, V., Burton, P., Danesh, J., Downey, P., Elliott,
956 P., Green, J., Landray, M., et al. (2015). UK biobank: an open access resource for
957 identifying the causes of a wide range of complex diseases of middle and old age.
958 *PLoS Med* 12, e1001779. 10.1371/journal.pmed.1001779.
- 959 64. Bycroft, C., Freeman, C., Petkova, D., Band, G., Elliott, L.T., Sharp, K., Motyer, A.,
960 Vukcevic, D., Delaneau, O., O'Connell, J., et al. (2018). The UK Biobank resource with
961 deep phenotyping and genomic data. *Nature* 562, 203-209. 10.1038/s41586-018-
962 0579-z.
- 963 65. Auton, A., Brooks, L.D., Durbin, R.M., Garrison, E.P., Kang, H.M., Korbel, J.O.,
964 Marchini, J.L., McCarthy, S., McVean, G.A., and Abecasis, G.R. (2015). A global
965 reference for human genetic variation. *Nature* 526, 68-74. 10.1038/nature15393.
- 966 66. Loh, P.-R., Tucker, G., Bulik-Sullivan, B.K., Vilhjálmsson, B.J., Finucane, H.K., Salem,
967 R.M., Chasman, D.I., Ridker, P.M., Neale, B.M., Berger, B., et al. (2015). Efficient
968 Bayesian mixed-model analysis increases association power in large cohorts. *Nature*
969 *Genetics* 47, 284-290. 10.1038/ng.3190.
- 970 67. Wu, Y., Burch, K.S., Ganna, A., Pajukanta, P., Pasaniuc, B., and Sankararaman, S.
971 (2022). Fast estimation of genetic correlation for biobank-scale data. *The American*
972 *Journal of Human Genetics* 109, 24-32. <https://doi.org/10.1016/j.ajhg.2021.11.015>.
- 973 68. Lee, J.J., McGue, M., Iacono, W.G., and Chow, C.C. (2018). The accuracy of LD Score
974 regression as an estimator of confounding and genetic correlations in genome-wide
975 association studies. *Genet Epidemiol* 42, 783-795. 10.1002/gepi.22161.
- 976 69. Wang, K., Li, M., and Hakonarson, H. (2010). ANNOVAR: functional annotation of
977 genetic variants from high-throughput sequencing data. *Nucleic Acids Res* 38, e164.
978 10.1093/nar/gkq603.
- 979 70. Purcell, S., Neale, B., Todd-Brown, K., Thomas, L., Ferreira, M.A., Bender, D., Maller, J.,
980 Sklar, P., de Bakker, P.I., Daly, M.J., and Sham, P.C. (2007). PLINK: a tool set for whole-
981 genome association and population-based linkage analyses. *American journal of*
982 *human genetics* 81, 559-575. 10.1086/519795.
- 983 71. Staley, J.R., Blackshaw, J., Kamat, M.A., Ellis, S., Surendran, P., Sun, B.B., Paul, D.S.,
984 Freitag, D., Burgess, S., Danesh, J., et al. (2016). PhenoScanner: a database of human
985 genotype-phenotype associations. *Bioinformatics (Oxford, England)* 32, 3207-3209.
986 10.1093/bioinformatics/btw373.
- 987 72. Kamat, M.A., Blackshaw, J.A., Young, R., Surendran, P., Burgess, S., Danesh, J.,
988 Butterworth, A.S., and Staley, J.R. (2019). PhenoScanner V2: an expanded tool for
989 searching human genotype-phenotype associations. *Bioinformatics (Oxford, England)*
990 35, 4851-4853. 10.1093/bioinformatics/btz469.
- 991 73. Hemani, G., Zheng, J., Elsworth, B., Wade, K.H., Haberland, V., Baird, D., Laurin, C.,
992 Burgess, S., Bowden, J., Langdon, R., et al. (2018). The MR-Base platform supports
993 systematic causal inference across the human phenome. *eLife* 7, e34408.
994 10.7554/eLife.34408.

- 995 74. Bowden, J., Davey Smith, G., and Burgess, S. (2015). Mendelian randomization with
996 invalid instruments: effect estimation and bias detection through Egger regression.
997 *Int J Epidemiol* 44, 512-525. 10.1093/ije/dyv080.
- 998 75. Bowden, J., Del Greco, M.F., Minelli, C., Davey Smith, G., Sheehan, N.A., and
999 Thompson, J.R. (2016). Assessing the suitability of summary data for two-sample
1000 Mendelian randomization analyses using MR-Egger regression: the role of the I2
1001 statistic. *Int J Epidemiol* 45, 1961-1974. 10.1093/ije/dyw220.
- 1002 76. Hartwig, F.P., Davey Smith, G., and Bowden, J. (2017). Robust inference in summary
1003 data Mendelian randomization via the zero modal pleiotropy assumption. *Int J*
1004 *Epidemiol* 46, 1985-1998. 10.1093/ije/dyx102.
- 1005 77. Verbanck, M., Chen, C.-Y., Neale, B., and Do, R. (2018). Detection of widespread
1006 horizontal pleiotropy in causal relationships inferred from Mendelian randomization
1007 between complex traits and diseases. *Nature Genetics* 50, 693-698. 10.1038/s41588-
1008 018-0099-7.
- 1009 78. Sophie, C., Josephine, Y.C., Michael, C., Adrian, B., and Michael, I.T. (2016). Cross-
1010 sectional study of diet, physical activity, television viewing and sleep duration in 233
1011 110 adults from the UK Biobank; the behavioural phenotype of cardiovascular
1012 disease and type 2 diabetes. *BMJ Open* 6, e010038. 10.1136/bmjopen-2015-010038.
1013